Severity-Based Discrimination Among Mesoscale Convective System Environments from Radisonde Analysis

A Senior Honors Thesis

Presented in Partial Fulfillment of the Requirements for graduation with distinction in Geography in the undergraduate colleges of The Ohio State University

by

Ariel Cohen

The Ohio State University
June 2006

Project Advisors: Professors Jay S. Hobgood and Jeffrey C. Rogers, Department of Geography

The original version of this thesis was co-authored by the following individuals as a part of Ariel Cohen's participation in the National Weather Center Research Experiences for Undergraduates with the University of Oklahoma during the summer of 2005 at the Storm Prediction Center in Norman, Oklahoma:

Ariel E. Cohen

Atmospheric Sciences Program – The Ohio State University, Columbus, OH

Michael C. Coniglio

NOAA/National Severe Storms Laboratory, Norman, OK

Stephen F. Corfidi

NOAA/NWS/NCEP/Storm Prediction Center, Norman, OK

Sarah J. Corfidi

NOAA/NWS/NCEP/Storm Prediction Center, Norman, OK

ABSTRACT

The prediction of the strength of mesoscale convective systems (MCSs), in terms of their potential to produce severe winds at the surface, is of concern to operational meteorologists. This study discusses meteorological variables derived from proximity soundings that are found to discriminate among long-lived severe wind producing MCSs known as derechos (DCSs), severe but non derecho-producing MCSs (SCSs), and weak MCSs (WCSs). These variables have been grouped into three categories: kinematics, instability, and moisture. Two-hundred sixty-nine warm season MCSs were rated based on intensity, and the stage of each system within the typical MCS life cycle. Decaying and dissipating MCSs were removed from the data set to focus on the most intense stages of the MCS life cycle. Variables were calculated from proximity soundings associated with each MCS, and statistical analyses were performed on these calculations. System-relative inflow and mid-level environmental lapse rates were found to be variables that discriminate among all three MCS environments. On the other hand, CAPE only discriminates well between WCS and SCS and between WCS and DCS environments. Mean mid- and upper-level wind speeds increase with increasing MCS severity, while low-level shear does not. Knowledge of the variables affecting MCS intensity permits improved forecasts and warnings of convective wind events.

1. Introduction

Organized clusters of thunderstorms meeting particular spatial and temporal requirements are known as mesoscale convective systems (MCSs) (e.g. Zipser 1982; Hilgendorf and Johnson 1998; Parker and Johnson 2000). Knowledge of the environmental parameters that govern MCS intensity is essential in operational meteorology. This is especially true of long-lived convective systems produce widespread damaging surface winds (derechos).

One of the first detailed examinations of derecho-producing convective systems (DCSs) was produced by Johns and Hirt (1987), who examined 70 warm season (May-August) MCSs between 1980 and1983. The study discussed the relationship between DCS position, motion, synoptic scale boundaries, and environmental parameters. They focused on the instability, moisture, and kinematic fields around DCSs, as well as characteristics of the distributions of these variables.

Coniglio et al. (2004) studied a suite of variables similar to those examined by Johns and Hirt (1987), but specifically used proximity soundings to determine characteristics of DCS environments. They took into account the various stages of a typical DCS's life cycle, as well as the synoptic-scale forcing patterns that support DCSs. The environmental conditions associated with a particular class of MCSs, known as mesoscale convective complexes (MCCs), have been thoroughly analyzed in Maddox (1983) and Maddox et al (1986). Both studies describe environments supporting MCCs, with emphasis on the synoptic scale.

Although these recent studies shed light on the environments of derechos, and others have discussed the environments of MCSs in general (e.g. Anderson and Arritt 1998, Liang and Fritsch 2000), there has not been a specific and thorough investigation into the differences in the environments of MCSs of different intensities. To build on this work, we present a study of the

variables that discriminate among weak MCSs, severe but non derecho-producing MCSs, and DCS environments. The purpose of the present work is to examine the differences in meteorological variables derived from proximity soundings among three categories of MCS intensity and to discuss the physical implications, which will in-turn provide forecasters with better information in the issuance of convective watches, mesoscale discussions, and short-term forecasts. Section 2 provides additional information on background work related to MCS. Section 3 describes the data set of MCSs considered in this study and the scheme used to rate the MCSs in the data set. Statistical analyses applied to the data set are discussed in Section 4. Sections 5, 6, and 7 describe the kinematic, instability, and moisture variables, respectively, found to discriminate the MCS environments. Finally, results are summarized in section 8.

2. MCS and DCS Literature Review

A detailed summary of current knowledge on MCSs is provided by Fritsch and Forbes (2001). Not only are MCSs responsible for widespread severe weather incidents, but they also play an important part in the hydrologic cycle of the world, as they are responsible for numerous heavy rain and flash flood events. MCSs usually initiate in the late afternoon or evening as distinct thunderstorm cells, sometimes even supercells, before congealing into large-scale organized thunderstorm structures, including areas of stratiform clouds and precipitation, as well as areas of moist convection. The average aerial extent of an MCS is in the range of hundreds of thousands of square kilometers, while time scales are on the order of at least six hours.

Maddox (1986) reveals that at least one injury or death is reported in approximately one MCS of every four MCCs. MCCs generally follow the mean mid- and upper level winds (Maddox 1986; Corfidi 2003). MCC intensity and duration was strongly modulated by the

location and strength of the nocturnal low-level jet stream, as well as any baroclinic zones around the MCC. Particularly relevant to this study was the finding that MCC strength is also enhanced by a vertical gradient in theta-e (θ_e): high theta-e air at low levels feed the MCCs, and low theta-e air exists at mid levels, allowing for enhanced downdrafts and outflow. Maddox (1983) presents an objective analysis of the composite environment of ten MCCs. A key characteristic in the environments of mature MCCs is lower tropospheric inflow. MCCs decay in regions of lower instability, and especially where the contribution of low-level warm air advection to instability slackened. Both Anderson and Arritt (1998) and Liang and Fritsch (2000) came to similar conclusions with regards to the impact of the low-level jet, moisture distributions, and instability associated with MCCs. According to Fritsch and Forbes (2001), the largest MCSs are actually MCCs, and MCCs are primarily nocturnal, with peak cold cloud shields occurring just after midnight local time. Additionally, most severe weather with MCCs occurs in the early portion of MCC life, with heavy rains and flash flooding threats increasing toward the latter portions of MCC life as distinct mesoscale circulations form and the environment around the MCC has had time to become more moist.

Fritsch and Forbes (2001) categorize MCCs into two types. Type-1 events involve the ingestion of parcels from an elevated layer on top of a stable surface layer, and thus occur on the cool side of a baroclinic zone. Lift in type-1 environments is accomplished through overrunning across the baroclinic zone. On the other hand, type-2 events involve ingestion of surface-based parcels located in a well-mixed layer, and occur in more barotropic environments than type-1 events. The moist downdrafts and associated cold pools in type-2 environments are responsible for further lifting and organization of convective overturning. Any vertical wind shear and associated hydrodynamic pressure perturbations are important for enhancing of lift in type-2

environments, which, unlike type-1 environments already exhibit vertical shear. In both types of events, the distinct MCS structure is dependent on saturation of a broad, deep layer of conditionally unstable air. Additionally, synoptic-scale features present in both types of events include low-level jets, warm air advection in low levels, and weak mid-level shortwaves.

Typical organization of MCSs is also described in Fritsch and Forbes (2001). Specifically, most MCSs are made up of elements of deep convection often organized in lines, especially in type-1 events, and an associated area of stratiform clouds and stratiform precipitation. Severe weather and flash flooding occur in convection areas, while lighter rainfall occurs in stratiform areas.

Movement of MCSs is the result of both an advective component of motion and cell propagation (Fritch and Forbes 2001; Corfidi 2002). The advective component is linked to mean wind velocity in the cloud layer, while the propagation component is linked to the velocity and magnitude of the inflow of high theta-e air, responsible for enhancing deep convective overturning. Thus, Fritsch and Forbes (2001) propose the difference between the mean cloud-layer wind velocity and the velocity of the low-level jet as a proxy for net MCS motion. On the other hand, Corfidi (2002) describes the net MCS motion as being the sum of the mean cloud-layer wind velocity and a cell propagation vector for MCSs that are backward-propagating, and twice the sum of the mean cloud-layer wind velocity and a cell propagation vector for MCSs that are forward-propagating.

MCSs also leave a lasting impact on the atmosphere, which extends well beyond the time of dissipation of the convection. Specifically, a mid-level mesovortex, a mesohigh due to a cold pool in low levels, and an upper-level anti-cyclone have been noted after MCSs affect a given region. These features are the result of two structures, which are in balance: positive potential

voriticty anomalies at midlevels and negative potential voriticty anomalies around the tropopuase. The positive anomaly often initiates new MCSs that produce heavy rain and flash flooding, as soils had already been saturated from the previous MCS.

MCSs that meet particular requirements of extended duration and produce widespread damaging surface winds are DCSs. Johns and Hirt (1987) study the environments associated with DCSs suggesting that relatively strong mean mid- and upper-level wind speeds are associated with them. Two important factors for the development of strong downdrafts are identified. They include a strong hydrolapse within the mid-troposphere (i.e. 3-7 km above ground level) to create enhanced negative buoyancy within the downdraft through entrainment of dry environmental air and the associated evaporation of precipitation, as well as the movement of high velocity air aloft to the surface. Additionally, large convective instability and the presence of dry air at mid levels lying above moist air in the low levels are characteristics common to many DCS environments. The dry-over-moist moisture profiles allowed for the development of large negative buoyancy in the lower levels that fostered development of strong downdrafts and severe surface winds (Johns and Hirt, 1987). Low level moisture also decreases the height of the level of free convection, allowing less low-level forcing to promote the continuation of deep convection.

Johns and Hirt (1987) find that DCSs were usually located in the vicinity of an east-to-west and nearly stationary baroclinic zone. This boundary provides the necessary horizontal temperature gradient that contributes to low-level warm air advection given winds at a nonzero angle to the boundary. This warm air advection is associated with uplift from the Omega Equation. Thus, relatively intense convection was often found to occur along or in the cool side of the boundary, usually to its north.

The dynamics associated with the gust front of an east-to-west moving DCS are also studied in Johns and Hirt (1987). After the DCS has formed, a mesohigh forms with a gust front radiating out of the mesohigh. The gust front travels quickly in the direction of the mean flow, because convergence and momentum transfer from the lower and middle troposphere is largest in the downwind direction of mesohigh and this flow is a good proxy for mean flow steering the DCS. Furthermore, convergence is enhanced downwind of a mesohigh when there is any easterly component of low level flow on the north side of the baroclinic zone.

Characteristics of progressive DCSs are also studied in Johns and Hirt (1987). On average, progressive DCSs are found to move around 15° to the right of the mean wind, indicating a component of motion into the higher-instability environment in the warm sector. They also provide information of one particular progressive derecho that occurred on 19 and 20 July 1983. Much of this particular DCS existed in the colder air mass, to the north of the baroclinic zone. Warm air advection into the cold air mass was responsible for lifting the convectively unstable air in that region. The warm air advection was found to exist up to 700 mb, allowing the level of free convection to be reached. This DCS moved from west to east and experienced weaker convective inhibition as it traveled across the northern Great Plains. Thus, the system expanded to the south toward the baroclinic zone and then, over time, became immersed within the warm sector.

Coniglio et al. (2004) study the various environments associated with different stages of a DCS's life. Specifically, they find that DCSs tend to mature as they move into moister low-level environments while retaining relatively dry conditions in mid-levels, which further establishes the importance of a dry-over-moist profile for sustaining DCSs. Additionally, DCSs are usually in their decaying stages when they move into environments with less CAPE. They also

emphasize that shear often extends through a large depth as DCSs mature, and that it weakens as DCSs decay. In particular, DCSs decay when they moved into areas with smaller 0–5- and 5–10-km shear, but no significant differences are found for the shear in the 0-1 km and 0-2.5 km layers. However, when synoptic scale forcing is found to be weak, DCSs tend to decay as they entered environments with smaller low-level shear. Additionally, Coniglio et al. (2004) find that DCSs commonly exist in environments with "straight-line" hodographs within all types of synoptic-scale forcing. Additionally, it is found that strong, low-level storm-relative inflow has an impact on the type, intensity, and duration of DCSs in weakly-forced synoptic scale environments, which confirms the findings in Evans and Doswell (2001). It is also found in Coniglio et al. (2004) that MCSs tend to exist in their weakening stages in areas of lower vertical gradient of θ_e, though the statistical confidence in this result is lower.

Evans and Doswell (2001) also emphasized that the convective available potential energy (CAPE) and vertical wind shear vary widely among DCS events. In cases when synoptic-scale forcing is stronger, mean wind speeds and shear throughout deep layers were stronger, while instability is much smaller than in inactive synoptic-scale environments. Thus, DCSs occur in areas with low CAPE and downdraft CAPE (DCAPE) when in the vicinity of a high-amplitude, mid-level trough and its associated surface cyclone. In these cases, instability plays little role in the creation of damaging and widespread surface winds, and strong downdrafts and strong cold pools are not necessary for severe surface winds. Rather, strong system-relative winds in the low-levels and weak system-relative winds at mid-levels were important to DCS development through their effects on the speed of movement. Additionally, shear within 6 km of the surface is important for DCS organization. In cases where synoptic-scale forcing is weak mean wind

speeds are relatively small and if instability is larger, the creation of strong downdrafts and cold pools are responsible for severe surface winds.

The reporting of severe surface winds is important for documentation and categorization of MCSs. Weiss et al. (2002) discuss problems with the reporting and archives of severe wind events based on reports from 1970 and 1999. In particular, the number of severe wind reports has increased significantly, with the proportion of severe wind events containing a maximum gust value increasing from 22% to 56% from 1995 to 1996, respectively. Weiss et al. (2002) discuss the problems with reports of severe winds, which are usually provided by humans. These problems arise from the many difficulties in estimating of wind speed and are likely responsible for the changing quality of the severe wind database. Dataset quality is of the utmost importance when focusing on the characteristics of severe-wind producing convective systems. Recommended methods to increase the precision of severe wind reports are suggested by Weiss et al. (2002) and Weiss and Vescio (1998). For example, each severe wind report could be labeled as measured or estimated, and / or any damage could be quantified based on a subjective, categorical scale. Weiss et al. (2002) stress the potential problem of providing misleading or inaccurate conclusions in a study if the severe wind reports are analyzed without regard to poor quality data in the severe wind database.

3. MCS Data set and MCS Intensity Rating Scheme

Using archived radar images provided by the University Corporation for Atmospheric Research (UCAR) and the Storm Prediction Center (SPC) (available online at http://locust.mmm.ucar.edu/case-selection/ and http://www.spc.noaa.gov/exper/archive/events), 269 MCSs were identified for this study that had an associated proximity sounding from upper

air observations. Each MCS exhibited a nearly contiguous line of leading convection at least 100 km long for at least five continuous hours. These MCSs occurred east of the Rocky Mountains between May and early September from 1998 through 2004. The MCSs were selected if the nearest part of the 50 dBZ radar reflectivity contour of the MCS was no more than 200 km and three hours removed from an observed sounding. The data were examined to verify that none of the soundings were contaminated by convection.

Following the above preliminary work, each system was categorized as a weak MCS (WCS), a severe but non derecho-producing MCS (SCS), or a DCS. Since this study focuses on convective systems that produce severe convective winds (wind gusts ≥ 50 knots or, in some cases, wind damage), we did not consider the occurrence of tornadoes or hail. The MCSs were categorized using storm reports from both Storm Data (NCDC) and the SPC database. Composite radar images from the aforementioned UCAR archive were used to verify that the severe wind reports were a result from the MCS in question. For all 269 MCSs, the number of severe wind reports produced by the MCS was determined using the SeverePlot program (Hart and Janish 1999), which displays the finalized dataset from NCDC. Since 2004 data were not yet available to SeverePlot at the time of classification, preliminary storm reports archived by the SPC (available online at http://www.spc.noaa.gov/climo) were used to perform the same classification process for that year.

As was discussed earlier, we recognize that some of the MCSs may have been under- or over-estimated in intensity due to population biases, inaccurate reporting, and/or a lack of *measured* severe wind events in the severe weather database (Weiss et al. 2002). However, the NCDC database provides the only means to produce climatological studies of this type, and we

assume that there is enough fidelity in this data to separate the weaker, shorter-lived systems from the intense, long-lived systems.

Several of the criteria for classifying the MCSs, especially for the identification of DCSs, were adapted from the discussion provided in Coniglio et al. (2004). For an MCS to be classified as an SCS or as a DCS, it must have produced at least six severe wind reports from the same MCS. If an MCS did not meet this criterion, it was classified as a WCS. The selection of six reports as a break point reflects the procedure for verification of Severe Thunderstorm Watches issued by the Storm Prediction Center. Specifically, if there are at least six reports of wind damage or thunderstorm wind gusts in excess of 50 knots, then a Severe Thunderstorm Watch is considered to be verified. Severe Thunderstorm Watches may be verified based on an appropriate number of hail reports, too, but those cases are not relevant to this study. This selection was made in this study, in order to be of most benefit to severe thunderstorm forecasters, as well as to provide a balanced subset of MCS intensities. By doing so, we are implicitly assuming that the true distribution of MCS intensities is smooth, meaning that there is no natural separation between a "weak" and "severe" MCS. This study is restricted to the analysis of quantitative differences. Severe wind events that can be distinguished from one another only by qualitative means are not captured in this analysis.

Three criteria were used to define a DCS: (1) there were at least six severe wind reports produced by the MCS, (2) successive severe wind reports occurred within three hours or 250 km of each other in a chronological progression, and (3) the major axis of the line connecting the initial and final severe wind reports was at least 400 km long. If all of these criteria were not met, the system was classified as an SCS. Fig. 1 shows sample wind damage and severe wind

gust report distributions produced by a WCS, an SCS, and a DCS. These distributions were generated from SeverePlot.

At the time of the proximity sounding, the appearance and trends of the radar reflectivity data were used to assess the mean speed and direction of the leading-line MCS motion near the sounding time, as well as the stage of the MCS in its life cycle. The stage of the MCS lifecycle surrounding the time of the observation is important, since the environments associated with weakening MCSs are quite different that the environments during their earlier stages (Coniglio et al. 2004). The four life cycle stages considered in this study were (1) initial cells prior to MCS development, (2) mature MCS, with strengthening or quasi-steady high reflectivity (50 dBZ or higher), (3) decaying MCS, with significantly weakened or shrinking areas of high reflectivity, and (4) dissipating MCS, with loss of system organization and associated areas of high reflectivity. Figs. 2, 4, 5, and 6 show each of four radar images illustrating each of the four life cycle stages for a DCS that developed in southwest Kansas, tracked across all of Oklahoma and Louisiana, and later entered the Gulf of Mexico on Thursday, June 16, 2005. Fig. 3 shows a photograph of the DCS corresponding to the radar image in Fig. 2. The picture was taken around 15 miles northwest of Slapout, Oklahoma, in Beaver County, Oklahoma, and the picture-taker was facing southwest Kansas.

MCSs that were decaying or dissipating around the time of the sounding are removed from the data set to focus on systems that were in the more intense stages of development. The quantities calculated from the proximity soundings in each category thus represent the collective conditions during MCS development and maturity. After the above two stratifications were made, a total of 49 WCSs, 87 SCSs, and 52 DCSs were selected. This data set should allow considerable confidence in the comparison of non-derecho and derecho environments despite the

relatively small number of DCS cases compared to WCS and SCS cases. The number of DCS cases may be relatively small due to too few severe wind reports in population-sparse areas.

4. Statistical Methods

Several hundred variables were calculated using the proximity sounding data that represented the kinematics, instability, and moisture environment of each MCS. Although substantial correlations exist among the variables, we did not want to make any prior assumptions about which of these variables are the best discriminators. Therefore, we focus on a handful of variables that are found to have the largest statistically significant differences among the MCS categories, as well as those variables that have been emphasized in previous studies. These variables include the following: mean speed within several layers, bulk shear within several layers, the angle between the MCS motion vector and the mean velocity vector within several layers, the angle between the MCS motion vector and the wind shear vector within several layers, several calculations related to CAPE, environmental lapse rate within several layers, the vertical difference in relative humidity in several layers, the vertical difference in equivalent potential temperature in several, and the precipitable water. A table listing a description and unit of measurement used for each of the variables considered is given in Table 1.

The 10^{th}, 25^{th}, 50^{th}, 75^{th}, and 90^{th} percentiles for each variable in each MCS category were calculated and displayed in box-and-whiskers plots to gauge relative magnitudes of each variable in each MCS environment. To help the reader gauge the significance of these differences between categories for each variable, absolute values of Z-Scores resulting from significance testing are displayed. The Z-Score is determined from the Wilcoxon two-sample rank sum

statistic, W (Hollander and Wolfe 1999) given a random sample of m observations, $X_1,\ldots,X_m$, from one population, and a random sample of n observations, $Y_1,\ldots,Y_n$, from another population. All of the values from the combined sample of the $m+n$ X-values and Y-values are ordered by magnitude from least to greatest. Each magnitude is then given an integer rank, from *1* to $m+n$ in order, with lower ranks corresponding to lower magnitudes and higher ranks corresponding to higher magnitudes. W is simply the sum of all the ranks assigned to the Y-values only. Mann and Whitney have proposed a statistic, U, similar to W, where U is the sum over all $m+n$ observations of the binary function $\varphi(X_i,Y_j)$, where

$$\varphi(X_i, Y_j) = \begin{cases} 1, \; if \; X_i < Y_j, \\ 0, otherwise. \end{cases}$$

Mann and Whitney have shown that, in the case of no ties, which is appropriate for this work, W and U are simply equal to one another except for an additive constant, such that

$$W = U + \frac{n(n+1)}{2} \; .$$

This implies that any tests based on U are equivalent to tests based on the Wilcoxon W statistic. Thus, a standardized normal variable is defined based on W. The Z-Score is computed for standardization, and is defined below:

$$Z = \frac{W - E_0(W)}{\{\mathrm{var}_0(W)\}^{1/2}} = \frac{W - \{n(m+n+1)/2\}}{\{mn(m+n+1)/12\}^{1/2}},$$

where Z is the standard normal version of W. Nonparametric tests like the Mann-Whitney test are attractive in this application since there is no a priori knowledge of underlying distributions for any of the differences studied here, which is required in the widely used student's t-test. For the Mann-Whitney test, it is assumed that the X's are a random sample from one population, the

Y's are a random sample from a second population, that the *X*'s and the *Y*'s are independent and identically-distributed, that the *X*'s and the *Y*'s are mutually independent or that the two samples are independent, and that the two populations are continuous populations. In this application, we define an absolute value of a Z-score above 1.645 (2.575), which corresponds to a probability of less than 10% (1%) that the two distributions were drawn from the same population, as indicating a "very good" ("excellent") discrimination between two categories.

5. Kinematic variables

This section discusses the differences in the mean wind and wind shear among the three MCS categories. For a given proximity sounding, mean winds are determined by taking the square root of the sum of the squared average u- and v-components of the wind at each standard and significant level within the layer under consideration. Within the upper troposphere (8-10 km and 8-12 km), mean winds are found to be excellent discriminators between SCS and DCS environments and between WCS and DCS environments (Figs. 7 and 8) according to the Z-Scores exceeding 2.575. Z-scores for both 8-10 km and 8-12 km mean wind speeds were especially high, ranging from around 2 between WCS and SCS environments, to around 4 between WCS and DCS environments. Our findings are not consistent with Johns and Hirt (1987). While they suggested that lower and middle tropospheric mean winds discriminate well between non DCS and DCS environments, our study indicates that mean upper tropospheric wind speeds are the best discriminators among MCS environments, and the differences in the environmental wind speeds between MCS environments drops off with decreasing height. Mean wind speeds in both the 8-10 km and 8-12 km layers were consistently found to range well above 20 m s^{-1} in DCS environments, and well below 27.5 m s^{-1} in WCS environments.

We also find that the MCS forward speed increases with MCS intensity (Figs. 9 and 10), with around 90% of the derechos exceeding 18 m s^{-1}. In discriminating between SCS and DCS and between WCS and DCS environments, the Z-score for MCS speed as a discriminator was found to be especially high, around 4.2 and 2.9, respectively. This provides quantitative evidence of the long-held notion that MCS severity is strongly related to the speed of the MCS. In fact, Corfidi (2003) assumed that the mean mid- and upper-level environmental winds are associated with increasing MCS forward speed and used a mean cloud-layer wind speed over a deep layer as an important component for assessing cold pool motion. Our findings support this assumption since mean mid- and upper-level environmental wind speeds in the present study were found to be linked with MCS severity (Figs. 7 and 8), and MCS severity is very strongly correlated with MCS speed.

The magnitudes of the bulk wind shear vectors are found to be largest in DCS environments (Figs. 11 and 12). The 0-6 km and 0-10 km mean shears are very good discriminators between SCSs and DCSs and between WCSs and DCSs. Figs. 11 and 12 show the results for the 0-4 km, 4-8 km, 8-12 km, 0-6 km, and 0-10 km layers. The utility of the shear variables is especially high when the layer through which the shear is distributed is deep. Among the entire set of shear variables, the 0-10 km shear is found to discriminate best among all three MCS environments, with median values of bulk shear around 22.5 m s^{-1} in WCS environments and over 30 m s^{-1} in DCS environments. However, wind shear in shallower layers, especially those near the surface (e.g. 0-4 km shear), was not found to be as good a discriminator as the 0-6 km and 0-10 km shears. In general, wind shear is not as good a discriminator as mean wind speed, as is indicated by the lower Z-scores for the shear variables.

The effect of wind shear on MCS intensity may be related to a conceptual model (Rotunno et al. 1988; Weismann and Rotunno 2004) describing the importance of environmental wind shear in the development and maintenance of quasi-linear MCSs. Model simulations indicated that, as low-level wind shear increases, the generation of upright convective cells is favored for longer time periods and initial cells become stronger. This occurs before enough horizontal vorticity generated by the cold pool causes the cells to tilt upwind. The results of this study are consistent with this idea, in the sense that MCS intensity was found to increase with increasing shear (Figs. 11 and 12). However, the observed magnitudes of the environmental low-level wind shear that were commonly found in this study to be associated with SCSs and DCSs may not be strong enough to suggest that the low-level shear/cold pool process described above is the dominant factor in controlling the MCS intensity. This finding is also discussed in Evans and Doswell (2001), Gale et al. (2002), and Coniglio et al. (2004). Stensrud et al. (2005) suggest that the large low-level shear values needed to produce persistent DCS structures do not occur regularly in the atmosphere as described in the idealized models. This point may be particularly important since observations from the BAMEX[1] field campaign suggest that cold pools are often stronger than what are typically produced in idealized models (Bryan et al. 2005).

Shear exists in a much deeper portion of the real atmosphere compared to the more confined layer used in the modeling studies, which formed the basis of Rotunno et al. (1988) and Weisman et al. (1988). Shear above the cold pool has been found to be important for maintaining stronger convection along the leading edge of the cold pool (Parker and Johnson, 2004; Coniglio et al. 2006). Results from the present study show that the effects of upper level shear alone may not be as important for determining the intensity of the system, since the 4-8 km

[1] BAMEX stands for the Bow Echoes and Mesoscale Convective Vortex (MCV) Experiment, which was a field program designed to obtain high-density kinematic and thermodynamic observations in and around bow-echo MCSs and mesoscale convective vorticies (Davis et al. 2004).

shear values are similar among the three MCS categories (Figs. 11 and 12). However, shear over a deep layer , such as the 0-10 km shear, which takes into account the benefits of low-level and upper-level shear, appears to be a better indicator of MCS intensity than either the low-level shear or upper-level shear alone (Figs. 11 and 12).

By comparing Figs. 7 and 11, it appears that mean-wind/cold pool comparisons may be more useful in assessing MCS intensity than wind shear/cold-pool comparisons, judging by the larger Z scores for the mean wind variables. However, the practical significance of these differences is not clear since the shear and the mean wind speed are correlated (Evans and Doswell 2001). In this study, the correlation coefficient between the 0-6 km mean wind and the 0-6 km wind shear is 0.674 for WCSs, 0.444 for SCSs, and 0.513 for DCSs. These moderate to strong correlations prevent a definitive statement on the relative physical importance of the mean wind versus the wind shear. However, from an operational standpoint, both the speed and shear of the mid and upper level winds provide useful information on the potential severity of the MCS.

The angle between the mean wind vector and the MCS motion vector was also investigated, since this is an indication of the propagation characteristics of the system. In this study, a positive angle indicates MCS motion to the right of the mean wind vector. This angle does an excellent job discriminating between WCS and SCS environments and between SCS and DCS environments for the 4-6 km, 4-8 km, and 0-8 km mean winds (Figs. 13 and 14). Median angles range in all three layers from just above 0° in WCS environments, to around 30° in SCS and DCS environments. Therefore, the MCS motion is more aligned with the mean mid- and upper-level wind vectors in WCS environments than in SCS and DCS environments. Section 5 discusses that measures of instability (e.g. environmental lapse rate and CAPE) indicate less

instability in WCS environments than in SCS and DCS environments. Thus, there is a stronger component of motion off the mean wind vector due to cell propagation into the more unstable air in SCS and DCS environments than in WCS environments.

The finding that DCS motion is generally parallel to the mean mid- and upper- level wind vector supports Corfidi (2003), which suggests the technique to determine the net MCS motion vector. This vector is the sum of the cell propagation vector and a vector representing the advective component of motion. This advective component of motion is taken to be either one times the mean cloud-layer wind vector for back-building MCSs, or two times the mean cloud-layer wind vector for forward-propagating MCSs (as DCSs often are). The mean cloud-layer wind vector is defined to be the 850-300 hPa mean wind in Corfidi (2003). As was noted earlier, the mean mid- and upper-level wind speeds were found to be largest in DCS environments. Thus, from Corfidi (2003), one would expect that DCSs move significantly faster than SCSs and WCSs. Indeed, we found that DCSs move almost 1.5 times as fast as SCSs and WCSs (Fig. 9).

Fig. 13 shows that the angle between DCSs and the mean mid- and upper-level winds is slightly smaller than the angle between SCSs and the mean mid- and upper-level winds. The larger mean mid- and upper-level wind vector in DCS environments would, according to Corfidi (2003), possibly explain the smaller angle between the MCS motion vector and the mean mid- and upper-level wind vectors. Specifically, the component of motion in the direction of the mean mid- and upper-level wind vector might be greater than the component of motion perpendicular to it, due to its large size in DCS environments.

DCSs were found in some cases to move faster than the mean wind speed in several layers of the atmosphere. This is likely due to the contribution of the component of the cell propagation in the direction of DCS motion vector. In some cases, portions of the MCS may

have experienced extremely large CAPE contributing to fast cell propagation, while CAPE measured from the proximity soundings may have not reflected particular geometries of CAPE. Because of this, it may be that the propagation vector dominates over the mean wind vector. So, the relative contributions of the two components of MCS motion cannot be gauged accurately in this study.

The wind shear vector over a deep layer (as approximated by the geostrophic thermal wind vector) has commonly been used as a proxy for forecasting the direction of MCS motion. The absolute value of the angle between the shear vector in several layers and the motion of an MCS was calculated and was found to be relatively small among all MCS environments. It was found to be a very good discriminator for the 0-6 km, 0-8 km, and 0-10 km shear vectors (Figs. 15 and 16) between the DCSs and the other MCS categories. In general, nonzero angles were found to exist between the shear vectors in these layers and the MCS motion vector. Median angles generally ranged from around 10° in WCS environments, to around 35° in SCS environments, to around 20° in DCS environments. This indicates that MCSs have a tendency to move at a small angle to the shear vectors in these layers. It is likely that this angle is often nonzero due to the effect of cell propagation on net MCS motion. The angle was found to be much smaller for DCSs, indicating that DCSs tend to follow the shear vector more closely than SCSs. This is completely consistent with the discussion regarding the relationship between mean mid- and upper-level wind speeds and wind shear. Fig. 17 shows two vectors overlaid on the Cartesian coordinate system, each corresponding to the 12 UTC proximity sounding from Topeka, Kansas on May 5, 1998 used to describe the environment of a DCS: the MCS motion vector, V_{MCS}, and the 0-6 km vector, $\delta_{0\text{-}6\ km}V$. The MCS moved at an angle of 30° to the right of north at a magnitude of 35.2 m s^{-1}. The 0-6 km bulk shear vector was only 1.25° to the left or to

the right of the MCS motion vector, with a magnitude of 28.14 m s^{-1}. Whether the MCS motion vector is to the right or left of the bulk shear vector is dependent on the horizontal distribution of other variables, including instability – the MCS will have a tendency to propagate into the more unstable air off the bulk shear vector. The angles between the shear vectors and the MCS motion vector were computed independent of orientation. Thus, the shear over a relatively deep layer is nearly parallel to the MCS motion vector.

Evans and Doswell (2001) identified the importance of system-relative inflow, especially in the 0-2 km layer, as a discriminator among non-derecho and DCS environments. Much of this relationship is attributed to the faster motion of DCSs over non-derecho-producing systems. The mean inflow winds are generally found to be slightly more than half of the MCS speed within each MCS severity level (cf. Figs. 7 and 18). This is confirmed by calculating the mean wind speed within the inflow layer in each sounding (Fig. 18). This suggests a strong relationship between system-relative wind and MCS speed, similar to what was found in Evans and Doswell (2001). However, calculation of the actual correlation coefficients between the MCS speed and the mean wind speed within the inflow layer, 0.634 for WCSs, 0.550 for SCSs, and 0.442 for DCSs, reveals only a moderate to strong relationship between the two variables, where the relationship decreases with increasing MCS severity. This drop off in correlation may be due to large variability in the speed of MCSs; some DCSs moved particularly faster than others, contributing to a larger spread of MCS speed in the DCS category. Since we found that MCS speed was an excellent discriminator among MCS categories, it is not surprising that mean system-relative inflow also is found to be a good discriminator among all three MCS environments (Figs. 18 and 19). The median of the absolute values of the mean inflow wind was found to drop from around 12 m s^{-1} in DCS environments to 8 m s^{-1} in WCS environments.

From each observed MCS speed and direction, storm-relative helicity in both the 0-1 km and 0-3 km layers was calculated. Storm-relative helicity in the 0-1 km and 0-3 km layers is found to be a poor discriminator among the MCS environments (Figs. 20 and 21), as might be expected. The range of helicity values experienced by the MCS within the dataset is large and generally similar among all MCS environments. This confirms that environments conducive to rotating updrafts are clearly not necessary for the development and sustenance of many MCSs, although MCSs and supercells certainly can coexist, as suggested by the 25th percentile of the 0-3 km helicity values extending to nearly 300 m^2 s^{-2} (Fig. 20).

6. Instability variables

As expected, several instability variables exhibit considerable skill in discriminating among the MCS environments (Figs. 22 through 25 and Figs. 30 through 33). In fact, instability variables appear to be the best discriminators, as their Z-scores are the highest, on average, of any tested in this study.

In this study, CAPE is calculated by lifting several parcels, including the surface parcel (SBCAPE), the most unstable single parcel (MUCAPE), and the parcel resulting from mixing the lowest 50 hPa, 100 hPa, and 150 hPa of the atmosphere (50 hPa, 100 hPa, and 150 hPa MLCAPE). Additionally, various measures of the maximum CAPE are found by mixing any 50 hPa, 100 hPa, and 150 hPa layer of the atmosphere (50 hPa, 100 hPa, and 150 hPa MU-MLCAPE). Note, for all the MU-MLCAPE quantities, only layers of air within the lowest 400 hPa of the atmosphere are candidates for being the most unstable layers. DCAPE is used to designate downdraft CAPE (Evans and Doswell 2001), which is calculated using a parcel that descends from the larger of two values: the height level of minimum equivalent potential

temperature and the wet-bulb zero height. None of the CAPE variables discriminate well between SCS and DCS environments, but all of the CAPE variables discriminate at very high levels between WCSs and SCSs and WCSs and DCSs (Figs. 22 through 25). The difference in median CAPE between WCS and SCS/DCS environments is largest for SBCAPE and MUCAPE, in which WCS environments experience median CAPEs ranging from around 1500 J kg^{-1} to around 3000 J kg^{-1} and from around 2000 J kg^{-1} to around 3000 J kg^{-1}, respectively. The MU-MLCAPE quantities do the best job of all the CAPE parameters in discriminating between SCS and DCS environments, with both the median 100 hPa and 150 hPa MU-MLCAPE decreasing by around 500 J kg^{-1} from DCS to SCS environments. However, the Z-scores are relatively low (between 1.0 and 1.6) indicating a relatively low confidence in this result.

As was previously indicated, CAPE on average is found to be smaller in DCS than in SCS environments. CAPE may fail to strongly discriminate between SCS and DCS environments in part because the data set included more DCSs that occurred in strongly forced environments with relatively small CAPE, which lowered the mean CAPE for the DCS category. The lack of a large difference in the CAPE variables between the SCS and DCS environments may also reflect the inability of a one-dimensional proximity sounding to detect differences in the spatial distribution of CAPE. However, CAPE alone does appear to provide some useful information on whether or not the MCS will produce severe winds, regardless of its longevity.

In order to understand the significance of a strongly-forced DCS in our dataset, it is important to consider the environment of one of these DCSs. An example of a DCS occurring in a strongly forced environment is one that moved across the Great Lakes region between August 22 and 23, 2000. The associated proximity sounding was taken from Detroit, Michigan (DTX) at 00 UTC on August 23, 2000. The lowest of the CAPE calculations was 180 J kg^{-1} for the 100-

hPa MLCAPE, and the highest was 450 J kg^{-1} for the MUCAPE, indicating meager CAPE supporting this DCS compared to that supporting the other DCS. The mean wind speeds in the 8-10 km and 8-12 km layers were around 35 m s^{-1}, indicating that that this DCS may have been supported in an environment with strong upper-level forcing, in which instability played a limited role in enhancing its severity (Evans and Doswell 2001).

Fig. 26 shows the 00 UTC radiosonde data from August 23, 2005 at Detroit. Instability was relatively marginal for an SCS or a DCS. However, mean mid- and upper-level wind speeds, as well as surface to mid- and upper-level wind shear is particularly strong, indicative of the potentially strongly forced environment in the vicinity of the DCS that moved across the Lower Michigan on August 22, 2005.

The surface observations across Lower Michigan at 00 UTC, as the DCS was exiting Lake Michigan into Lower Michigan, are found in Fig. 27. Low levels across Lower Michigan and ahead of the DCS were particularly moist (e.g. 79 °F temperature and 72 °F dewpoint temperature at Battle Creek, MI). There was probably greater instability to the west of Detroit, as the temperature and dewpoint at Detroit were 75 °F and 61 °F, respectively, indicating much drier low levels. This more stable air at Detroit may be due in part to the south-to-north advection of stable air across Lake Erie, per the southerly winds at Detroit at 00 UTC.

Fig. 28 shows the 300 mb isotachs at 2100 UTC on August 22, 2000. Divergence associated with the right-rear quadrant of the 90-knot jet streak across northeast Wisconsin and the southern Upper Peninsula of Michigan likely, as well as the strong shear associated with the 70 knots of west-northwesterly flow, likely contributed to the strongly-forced environment around the DCS. Fig. 29 shows the base-reflectivity radar data taken sampled by from Grand

Rapids, Michigan around 0204 UTC on August 23, 2005. At this time, the DCS was at its maximum intensity.

Evans and Doswell (2001) indicated that DCAPE can be used to approximate cold pool strength, as DCAPE is a measure of the potential for cold downdraft development. For the warm season-type environments examined in this study, it is likely that the cold pool is largely responsible for the system's sustenance. As such, we find that DCAPE increases with increasing MCS intensity (Figs. 24 and 25), as found by Evans and Doswell (2001). While differences in DCAPE between all three MCS categories show DCAPE to be a good discriminator, the actual difference in DCAPE, around 100 J kg^{-1}, may be too small to be of operational significance. However, the DCAPE differences are by far the most significant among the WCS and DCS categories.

Despite the fact that CAPE was found to be greater for SCSs than for DCSs and WCSs, the environmental lapse rate (γ) was found to be greatest for DCSs in the 2-4 km, 4-6 km, 4-8 km, 0-6 km, and 0-8 km layers (Figs. 30 and 31). The 2-4 km and 4-6 km environmental lapse rates both discriminate very well among all three MCS environments with Z-scores well above 1.645. Median environmental lapse rates range from 6.75 °C km^{-1} to just under 7.50 °C km^{-1} in both the 2-4 km and 4-6 km layers. The distinction is especially evident between WCSs and DCSs. However, with increasing layer-size, the utility of environmental lapse rate as a discriminator diminishes. Because environmental lapse rates, unlike CAPE, are usually considered in thin layers of the atmosphere, they are more likely to uncover small-scale instability features in the vertical that may be masked by CAPE. As a result, mid-level environmental lapse rates may generally be better discriminators than CAPE, at least from a one-dimensional perspective.

7. Moisture variables

The vertical difference in relative humidity (RH) between low and mid levels (1-5 km and 2-4 km) and the vertical difference in θ_e between low and mid levels (1-3 km, 1-5 km, and 1-7 km) are found to be excellent discriminators between WCS and both SCS and DCS environments (Figs. 32 and 33), similar to what was found for DCAPE. The vertical difference in θ_e was found to practically mirror the vertical difference in RH in the 1-5 km layer, but not in the 2-4 km layer. The vertical θ_e difference is found to be least negative for WCS environments and generally most negative for SCS and DCS environments. It is interesting that, by comparing Figs. 25 and 33, the 1-5 km and 1-7 km $\delta\theta e$ does a much better job discriminating between WCS and SCS environments than DCAPE. Of all the vertical moisture gradient variables, the 1-7 km vertical gradient of θ_e does the best job discriminating between WCS and DCS and between WCS and SCS environments. This vertical difference has a median that ranges from around -10 K in WCS environments to around -15 K in SCS and DCS environments.

A layer of the atmosphere with a negative gradient in θ_e is potentially, or convectively, unstable, as described by Schultz et al. (2000). Upon lifting a convectively unstable layer, a process that often proceeds MCS development, the temperature of the bottom of the layer decreases more slowly than does the temperature at the top of the layer (due to the higher moisture content and resulting lower saturated adiabatic lapse rate present at the bottom of the layer). The result is an increased environmental lapse rate within the convectively unstable layer, and potential convective formation and overturning. This increase in environmental lapse rate within the layer also leads to greater conditional instability within the layer.

However, since the vertical gradient of θ_e is a very good discriminator only between WCS and SCS environments and between SCS and DCS environments, a vertical gradient of θ_e is likely linked with any wind damage potential, regardless of its longevity, as suggested in Atkins and Wakimoto (1991) and Wakimoto (2001). There are two distinct physical processes associated with a large negative vertical gradient in θ_e related to the enhancement of severe surface winds: (1) the initial formation of deep, convection resulting from convective instability (Schultz et al. 2000), and (2) the effects on the downdrafts. The role of a vertical difference in θ_e is mainly to initiate the downdraft. The dry air at mid levels, marked by relatively low θ_e values, leads to entrainment of dry air into the downdraft. In a comparison with downdraft observations during the Joint Airport Weather Study (JAWS), Srivastava (1985) discusses that the downdrafts studied were indeed caused by evaporation. This causes a relative increase in downdraft density, since the density of dry air is larger than the density of moist air. However, too much evaporation can yield to the dry air mixing ratio within the downdraft to significantly increase, leading to warming closer to the dry adiabatic lapse rate, and thus enhanced decreased density. The effect on the downdrafts manifests itself in the development of negative buoyancy as precipitation falls through subsaturated air. In addition, if the downdraft can maintain saturation, the downdraft is enhanced as it encounters the relatively large virtual temperatures of the warm, moist low levels (Wakimoto 2001). Specifically, given a relatively moist and less dense environment at low levels, marked by a higher θ_e, the relative density difference between the descending parcel and its environment is enhanced (Proctor 1989). Thus, warm, moist low levels, yielding higher θ_e values, are more supportive of intense MCSs than warm, dry low levels, yielding lower θ_e values.

Srivastava (1985) and Proctor (1989) both point out several other factors in considering downdraft maintenance not specifically discussed in our study. Melting level height, average environmental lapse rate below the melting level, and the humidity at the melting level and 1 km above the surface are all related to downdraft maintenance. The finding of increased low level environmental lapse rate with increased MCS severity may be associated with the more negative vertical gradient in θ_e found in more severe MCS environments.

In MCS environments with nearly saturated thermodynamic profiles, θ_e varies much less with height, yielding smaller gradients in θ_e. In these nearly saturated profiles, the process of dry air entrainment and resulting evaporational cooling occurs less effectively. However, it is interesting that the precipitable water (PWAT) is found to be a very good discriminator between SCSs and DCSs (Figs. 34 and 35), despite the fact that the vertical gradient in θ_e is not a good discriminator between these two groups (Figs. 32 and 33). In DCS environments, median PWAT is around 1.3 inches, while it is around 1.5 inches in WCS and SCS environments. Since PWAT is smaller in DCS environments than in SCS environments, the overall moisture content in DCS environments is smaller than in SCS environments, which is likely the result of drier conditions in mid-levels. A possible explanation is that the larger lapse rates observed for the DCSs counter the lower integrated moisture content to produce similar vertical gradients in θ_e. In any case, these results suggest that the vertical gradient in θ_e could be used together with PWAT to help discriminate effectively between SCSs and DCSs. For example, mixing ratio could be integrated in various layers of the atmosphere to determine a form of PWAT in the various layers. Vertical differences in this integrated quantity could be calculated and compared against vertical differences in θ_e between various levels.

8. Summary and Conclusions

This study discusses several meteorological variables that are found to discriminate among the environments associated with different intensities of MCSs. Three MCS types are defined from a set of 269 warm season MCSs: weak MCSs (WCSs), severe but non derecho-producing MCSs (SCSs), and derecho-producing MCSs (DCSs).

Concepts presented in two papers [Corfidi (2003) and Evans and Doswell (2001)] were explored in depth in this study. Corfidi (2003) suggests that the advective component of MCS motion (represented by the mean cloud-layer wind) may be added twice to the propagation vector to obtain an estimate of the net motion of a forward propagating MCS. In light of the present study, this seems like a reasonable approach, since both MCS motion and mean wind speed were found to increase with increasing MCS intensity. Additionally, DCSs tended to move in a direction more parallel to the mean mid- and upper-level winds than SCSs and WCSs. As in Evans and Doswell (2001), system-relative inflow is positively correlated with MCS intensity. Additionally, the lack of utility of low-level shear in discrimination appears to be related to problems with the simulations presented in Rotunno et al. (1988) and Weismann and Rotunno (2004).

Variables that are positively correlated with MCS intensity and that are found to be the best discriminators include mid-level environmental lapse rates, mean mid- and upper-level winds, and deep-layer wind shear, to a lesser extent. With an understanding of these variables, forecasters will have a refined and more complete guide to forecasting MCS severity. Additionally, a composite of particular values of the variables presented in this study can be used to infer the strength of an MCS.

This study provided a description of the environments associated with severe wind-producing MCSs based on the analysis of numerous variables derived from sounding data. The results of this study need to be considered in the forecasting of the severity of convective wind events. For example, increases in environmental lapse rate at a given location signal indicate the potential for a more severe MCS. However, this study also has rejected some commonly held notions. Specifically, at a given location, CAPE should not be used solely in the prediction of MCS severity, as CAPE does not discriminate well between SCS and DCS environments. Additionally, we have confirmed other studies, showing that low-level shear is indeed a poor discriminator among the three MCS severity categories.

The variables examined may be used to describe the vertical structure of the atmosphere and the way that structure relates to MCS intensity. Combined with an understanding of how the horizontal distribution of these variables affects MCS development and evolution, one can gain a more complete understanding of the factors contributing to MCS intensity with the results produced in this study. Future work could include considering the impact of synoptic scale features, such as upper-level troughs and their associated upper-level divergence and positive vorticity advection, low level baroclinic zones, low level jets, etc., specifically on discriminating between the environments of different MCS intensities.

Acknowledgements

This material is based on work supported by the National Science Foundation under Grant No. 0097651.

The author thanks the personnel of the National Severe Storms Laboratory (NSSL) and the Storm Prediction Center (SPC) for their help with this project. He greatly appreciates the

review of an earlier version of this paper by Harold Brooks (NSSL) and related discussions with Charles Doswell III (CIMMS). The author would also like to thank David Bright (SPC) for his assistance in preparing computer accounts for this work. Additionally, this project would not have been possible without the care and attention of the author's mentors, Mike Coniglio and Steve and Sarah Corfidi, the author's professors, Jay Hobgood, Jeff Rogers and Jackie Miller, the author's dad, Joel Cohen, and the interest of the author's Meteorology 623.02 Spring Quarter 2006 students. Finally, the author thanks Daphne LaDue for her enormous efforts in running the National Weather Center Research Experiences for Undergraduates program.

Table 1

List of Variables, Their Meanings, and Units

"A-B km" denotes the layer bounded by the A-km level and the B-km level.

Symbol	Explanation	Units
A-B km $\lvert\vec{V}\rvert$	A-B km velocity vector measured in the reference frame of the proximity sounding vector magnitude	$m\ s^{-1}$
A-B km $\lvert\vec{\delta V}\rvert$	A-B km wind shear vector magnitude	$m\ s^{-1}$
A-B km α	angle between MCS motion vector and mean A-B km $\vec{V}$ measured counterclockwise from the direction of MCS motion	degrees
A-B km β	angle between MCS motion and A-B km $\vec{\delta V}$	degrees
SBCAPE	surface-based convective available potential energy (CAPE)	$J\ kg^{-1}$
MUCAPE	most-unstable CAPE	$J\ kg^{-1}$
50 hPa MLCAPE	lowest 50-hPa mixed layer CAPE	$J\ kg^{-1}$
100 hPa MLCAPE	lowest 100-hPa mixed layer CAPE	$J\ kg^{-1}$
150 hPa MLCAPE	lowest 150-hPa mixed layer CAPE	$J\ kg^{-1}$
50 hPa MU-MLCAPE	most-unstable 50-hPa mixed layer of the lowest 400 hPa CAPE	$J\ kg^{-1}$
100 hPa MU-MLCAPE	most-unstable 100-hPa mixed layer of the lowest 400 hPa CAPE	$J\ kg^{-1}$
150 hPa MU-MLCAPE	most-unstable 150-hPa mixed layer of the lowest 400 hPa CAPE	$J\ kg^{-1}$
A-B km γ	A-B km environmental lapse rate	$°C\ km^{-1}$
A-B km δRH	A-B km vertical difference in relative humidity	%
A-B km $\delta\theta_e$	A-B km vertical difference in equivalent potential temperature	°C
PWAT	precipitable water	in

References

Anderson, C. J. and R. W. Arritt, 1998: Mesoscale convective complexes and persistent elongated convective systems over the United States during 1992 and 1993. Mon. Wea. Rev., 126, 578-599.

Atkins, N. T., and R. M. Wakimoto, 1991: Wet Microburst activity over the southeastern United States: implications for forecasting. *Wea. Forecasting*, **6**, 470-482.

Corfidi, S. F., 2003: Cold pools and MCS propagation: Forecasting the motion of downwind-developing MCSs. *Wea. Forecasting*, **18**, 997-1017.

Coniglio, M. C., D. J. Stensrud, and M. B. Richman, 2004. An observational study of derecho-producing convective systems. *Wea. Forecasting*, **19**, 320-337.

Coniglio, M.C., L. J. Wicker, and D. J. Stensrud, 2006: Effects of upper-level shear on the structure and maintenance of strong, quasi-linear mesoscale convective systems. Accepted to *J. Atmos. Sci.*

Evans, J. S., and C. A. Doswell III, 2001: Examination of derecho environments using proximity soundings. *Wea. Forecasting*, **16**, 329-342.

Fritsch J. M. and G. S. Forbes, 2001: Mesoscale convective systems. *Severe Convective Storms*, *AMS Meteor. Monogr.*, C. Doswell III, Ed., **28**, Amer. Meteor. Soc., 323-357.

Gale, J. J., Gallus, W. A., Jungbluth, K. A. 2002: Toward improved prediction of mesoscale convective system dissipation. *Wea. Forecasting*, **17**, 856–872.

Gilmore M. S., and L. J. Wicker, 1998: The influence of midtropospheric dryness on supercell morphology and evolution. *Mon. Wea. Rev*., **126**, 943-958.

Hart, J. A., and P. R. Janish, 1999: SeverePlot: Historical severe weather report database. Version 2.0. Storm Prediction Center, Norman, OK. [Available online at http://www.spc.noaa.gov/software/svrplot2/.]

Hilgendorf, E. R., and R. H. Johnson, 1998: A Study of the evolution of mesoscale convective systems using WSR-88D data, *Wea. Forecasting*, **13**, 437-452.

Hollander, M. and Wolfe, D. A., 1999: Hypothesis Testing. *Nonparametric statistical methods*. John Wiley & Sons, Inc., pp. 108-109.

Image Archive, 2004. *University Corporation for Atmospheric Research.* [Available online at http://locust.mmm.ucar.edu/case-selection/.]

Johns, R. H., and W. D. Hirt, 1987: Derechos: Widespread Convectively Induced Windstorms. *Wea. Forecasting*, **2**, 32-48.

Liang, A.G. and J.M. Fritsch, 2000: The large scale environments of the global population of mesoscale convective complexes. *Quart. J. Roy. Meteor. Soc*., **123**, 389-405.

Maddox, R. A., 1983: Large-scale meteorological conditions associated with midlatitude, mesoscale convective complexes. *Mon. Wea. Rev.*, **111**, 1475--1493.

Maddox, R. A., K. W. Howard, D. L. Bartels and D. M. Rodgers, 1986: Mesoscale Convective Complexes in the Middle Latitudes. *Mesoscale Meteorology and Forecasting*, P.S. Ray, Ed., Amer. Meteor. Soc., 390- 413.

Parker, M. D., and R. H. Johnson, 2000: Organizational modes of midlatitude mesoscale convective systems. *Mon. Wea. Rev.,* **128,** 3413-3436.

Proctor, F.H., 1989: Numerical simulations of an isolated microburst. Part II: Sensitivity experiments. J. Atmos. Sci., **46**, 2143-2165.

Rotunno, R., J. B. Klemp, and M. L. Weisman, 1988: A theory for strong, long-lived squall lines. *J. Atmos. Sci.*, **45**, 463-485.

Schultz, D. M., P. N. Schumacher and C. A. Doswell III, 2000: The intricacies of instabilities. *Mon. Wea. Rev.*, **128**, 4143-4148.

Srivastava, R.C., 1985: A simple model of evaporatively driven downdraft: Application to microburst downdraft. *J. Atmos. Sci*., **42**, 1004-1023.

Stensrud, D. J., M. C. Coniglio, R. P. Davies-Jones, and J. S. Evans, 2005: Comments on "A Theory for Strong Long-Lived Squall Lines Revisited". *J. Atmos. Sci.*, in press.

Storm Prediction Center website. *Storm Prediction Center*. [Available online at http://www.spc.noaa.gov.]

Storm Reports. *Storm Prediction Center*. [Available online at http://www.spc.noaa.gov/climo/.]

Wakimoto, R. M., 2001: Convectively driven high wind events. *Severe Convective Storms, Meteor. Monogr*., No. 50, Amer. Meteor. Soc., 255-298.

Weisman, M. L., J. B. Klemp, and R. Rotunno, 1988: Structure and evolution of numerically simulated squall lines. *J. Atmos. Sci.,* **45**, 1990-2013.

Weisman, M. L., and R. Rotunno, 2004: "A Theory for long-lived squall lines" revisited. J. Atmos. Sci., **61,** 361-382.

Weiss, S. J., and M. D. Vescio, 1998: Severe local storm climatology 1955-1996: Analysis of reporting trends and implications for NWS operations. *Preprints,* 18th Conf. on Severe Local Storms, Minneapolis, Amer. Meteor. Soc., 536-539.

Weiss, S. J., J. A. Hart, and P. R. Janish, 2002: An examination of severe thunderstorm wind report climatology: 1970-1999. Preprints, *21st Conf. on Severe Local Storms*, San Antonio, TX, Amer. Meteor. Soc., CD-ROM, paper 11B2.

Wilks, D. S., 1995: Hypothesis Testing. *Statistical methods in the atmospheric sciences*. Academic Press, pp. 114-158.

Zipser, E. J., 1982: Use of a conceptual model of the life cycle of mesoscale convective systems to improve very-short-range forecasts. *Nowcasting*, K. Browning, Ed., Academic Press, pp. 191-204.

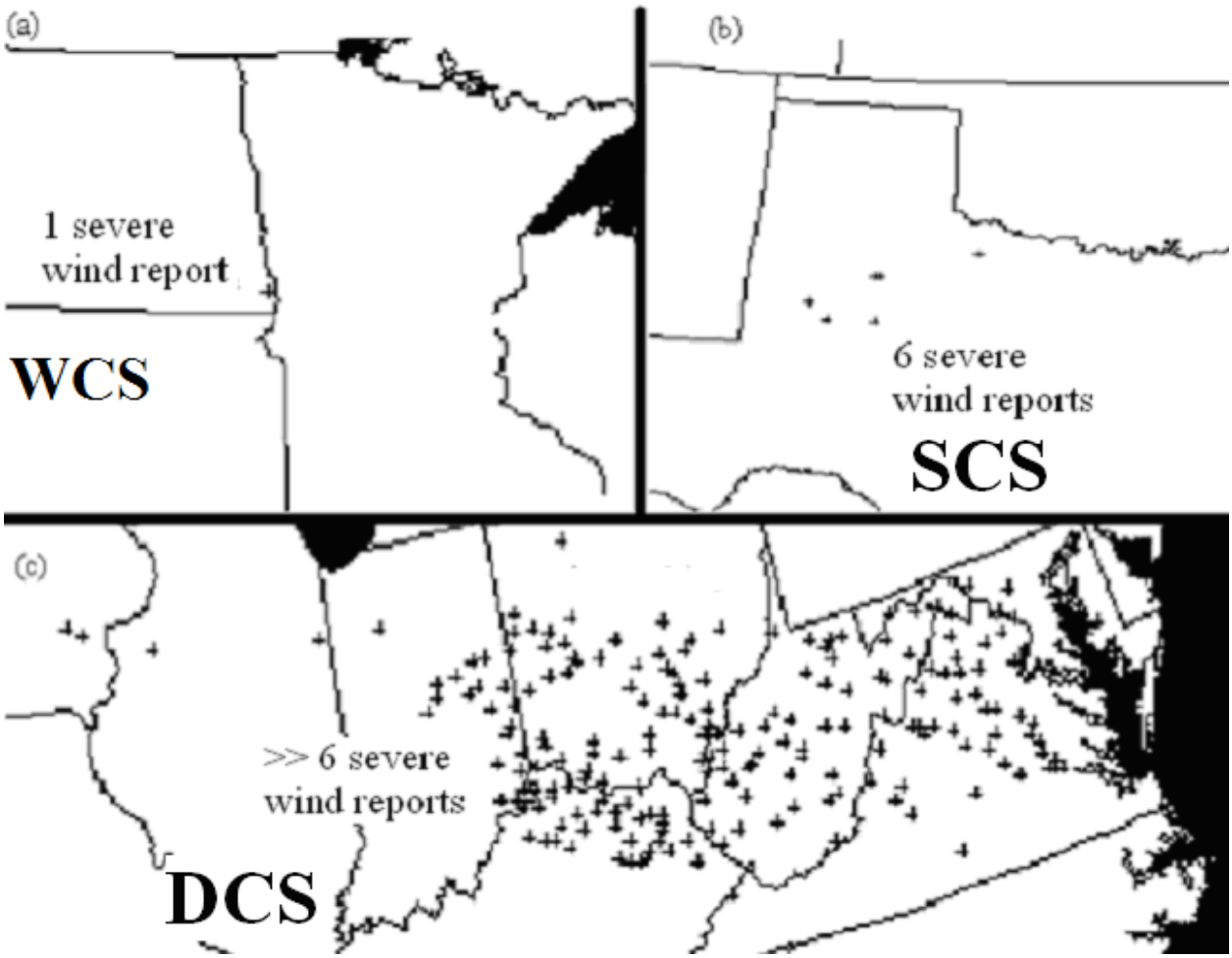

Fig. 1. (a) Wind damage and severe wind gust report distributions associated with (a) a WCS, (b) an SCS, and (c) a DCS.

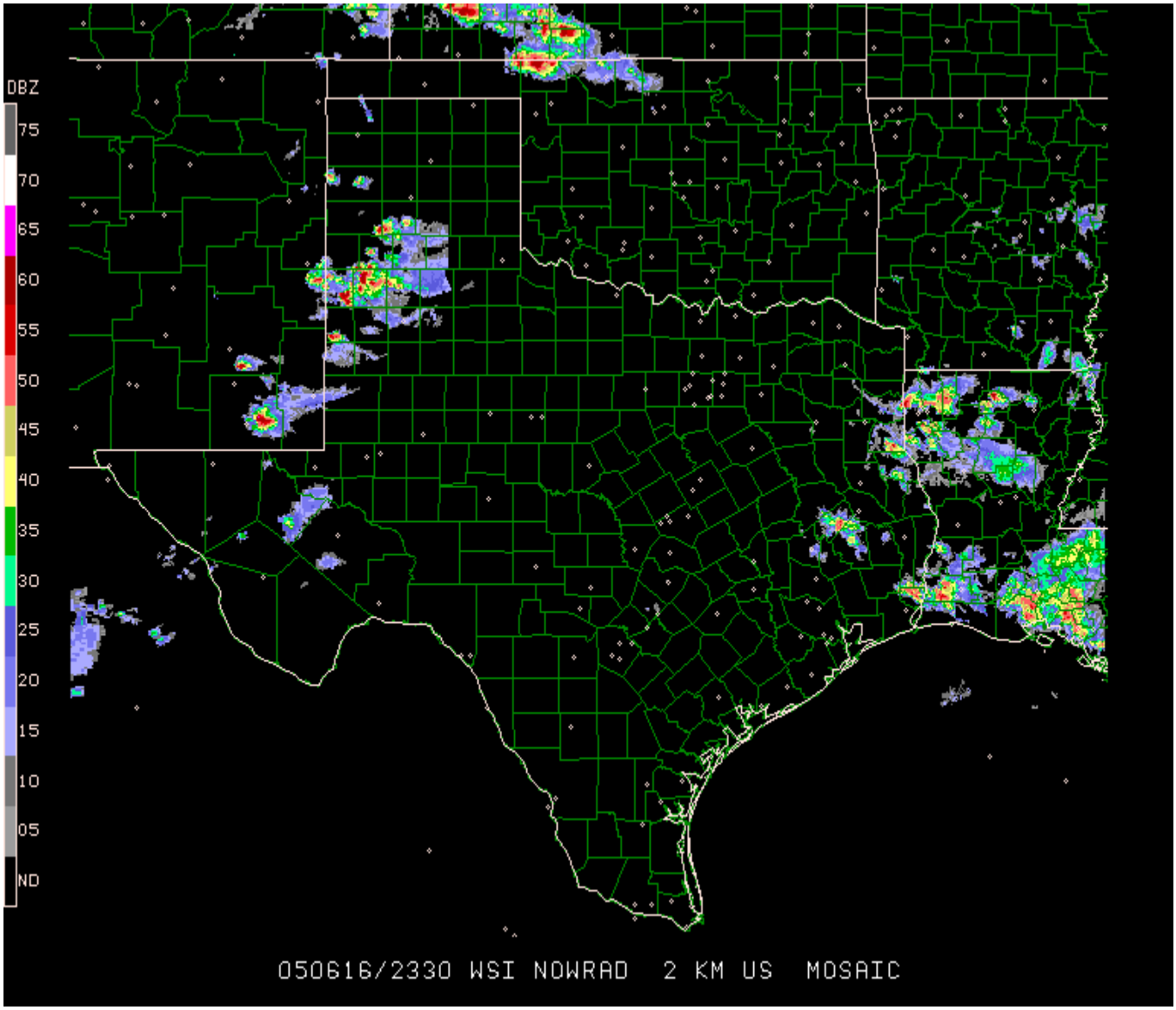

Fig. 2. Radar image corresponding to initial cells prior to MCS development.

Fig. 3. Picture of the DCS corresponding to the radar image in Fig. 2 taken around 15 miles northwest of Slapout, Oklahoma, in Beaver County, Oklahoma. The picture-taker was facing southwest Kansas.

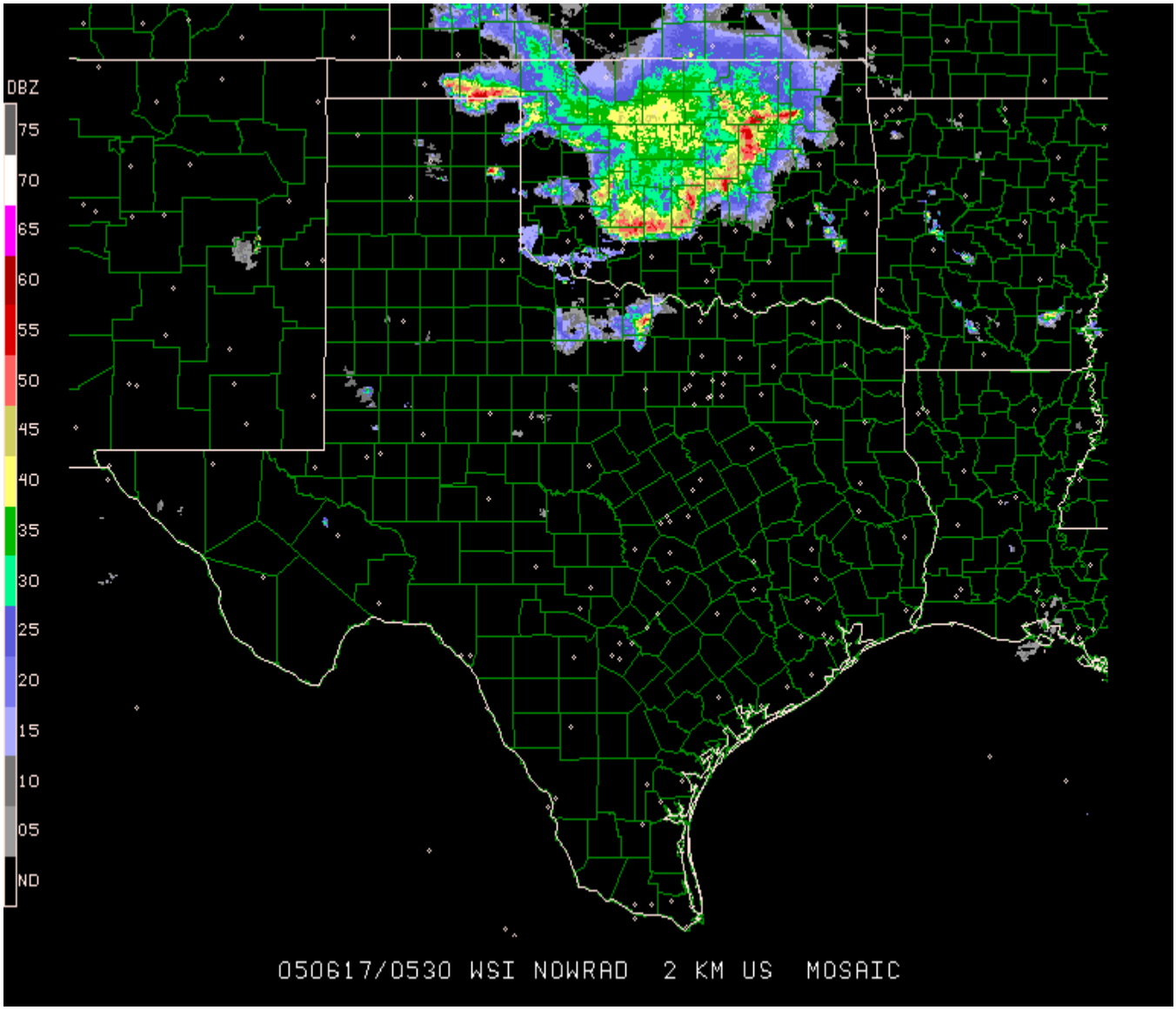

Fig. 4. Radar image corresponding to a mature MCS, with strengthening or quasi-steady high reflectivity (50 dBZ or higher).

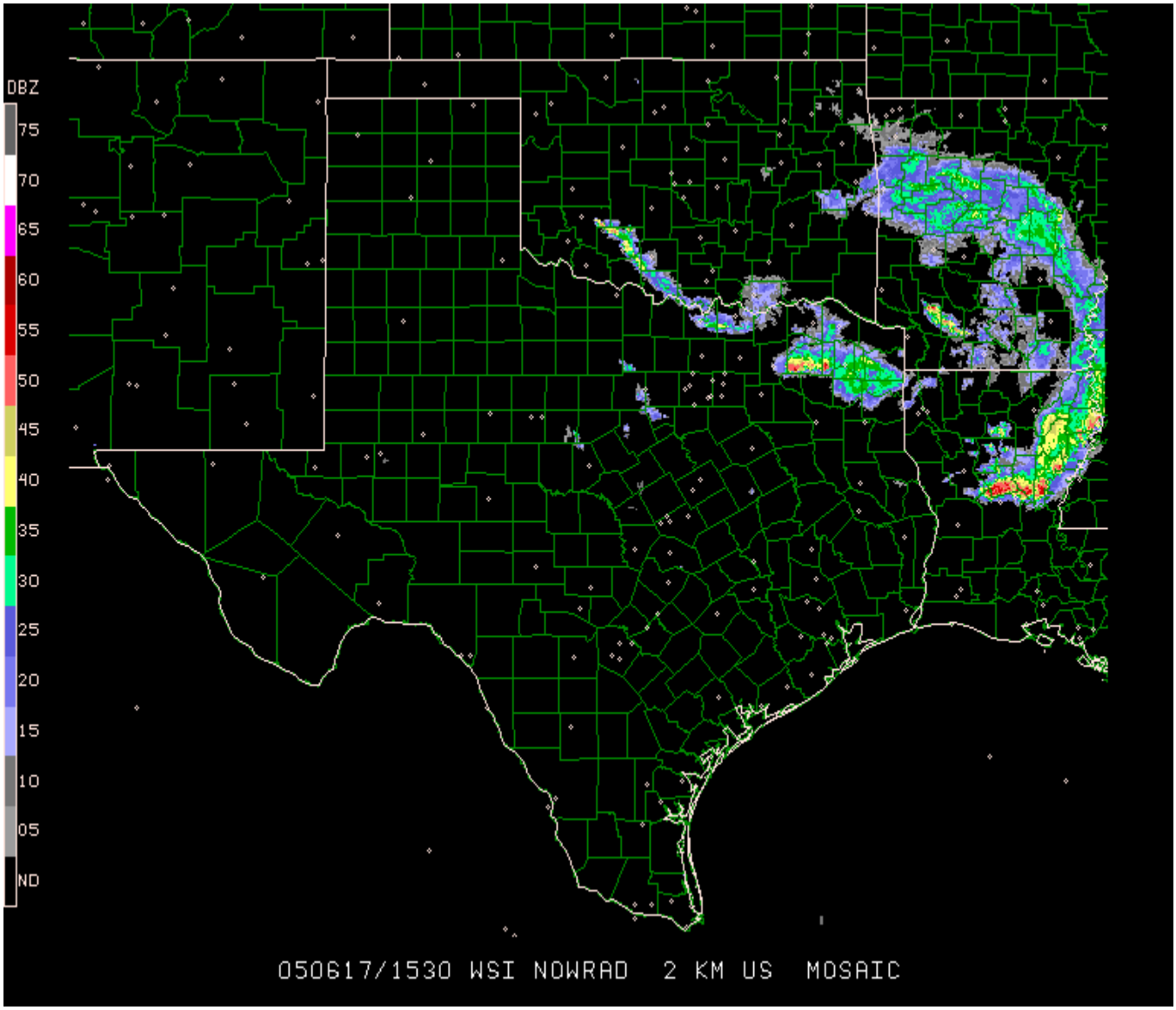

Fig. 5. Radar image corresponding to a decaying MCS, with significantly weakened or shrinking areas of high reflectivity.

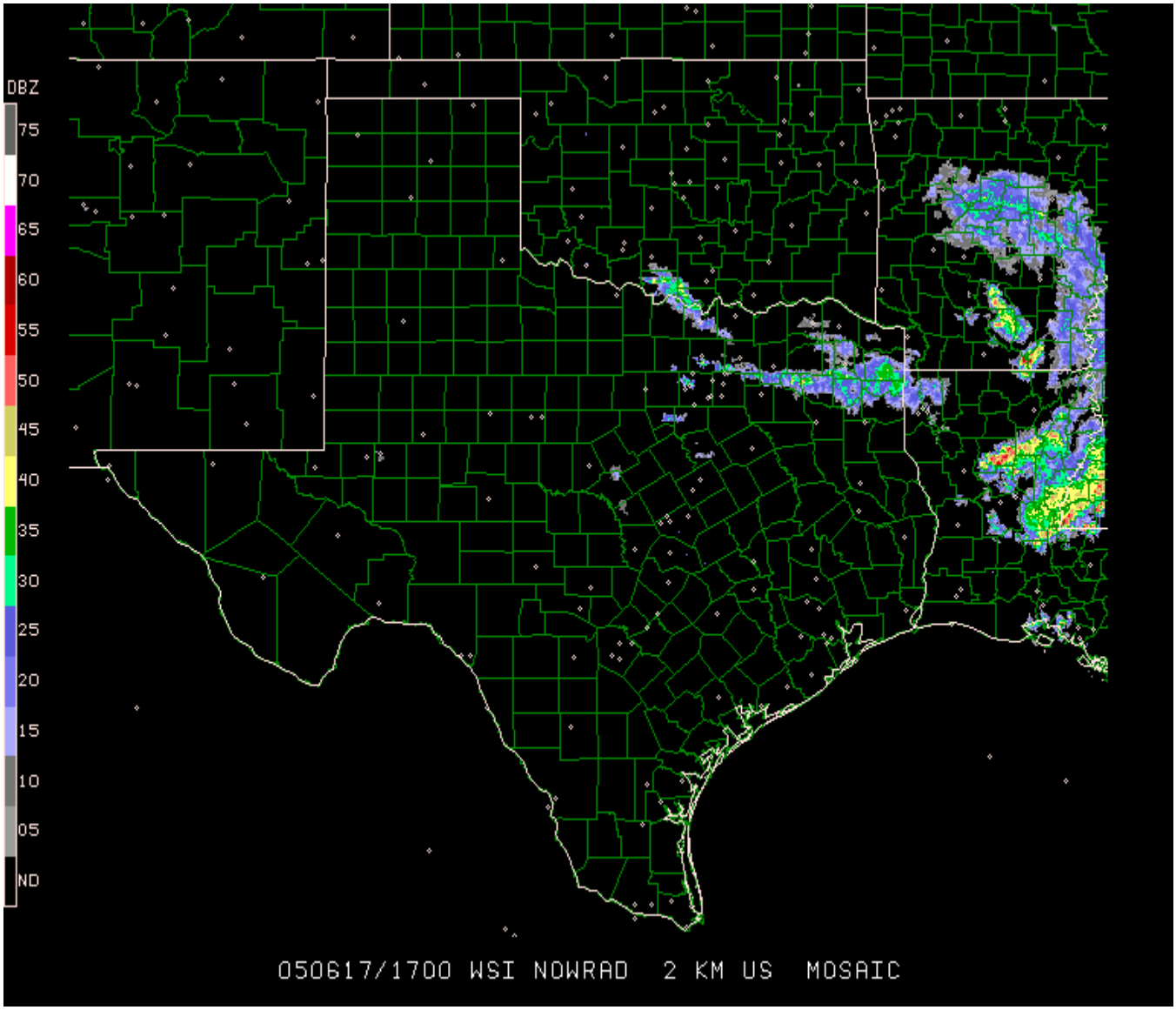

Fig. 6. Radar image corresponding to a dissipating MCS, with loss of system organization and associated areas of high reflectivity.

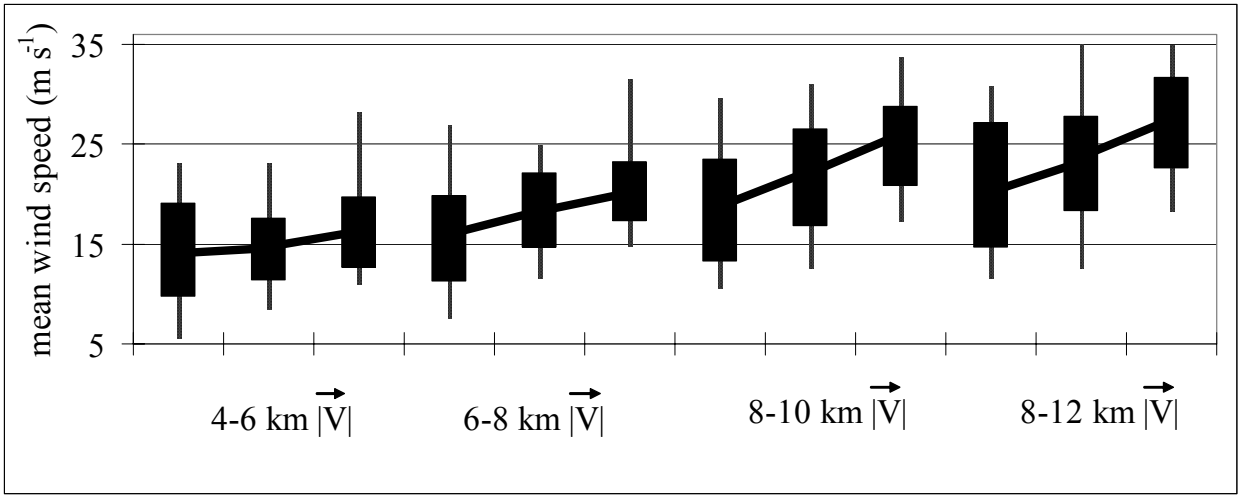

Fig. 7. Box-and-whiskers plots for the 4-6 km, 6-8 km, 8-10 km, and 8-12 km mean wind speed. Each set of three categories indicates the results for the WCSs, SCSs, and DCSs, from left to right. The bottom and top whiskers represent the 10th and 90th percentiles, respectively, the bottom and top of the boxes represent the 25th and 75th percentiles, respectively, and the connecting line represents approximately the 50th percentile.

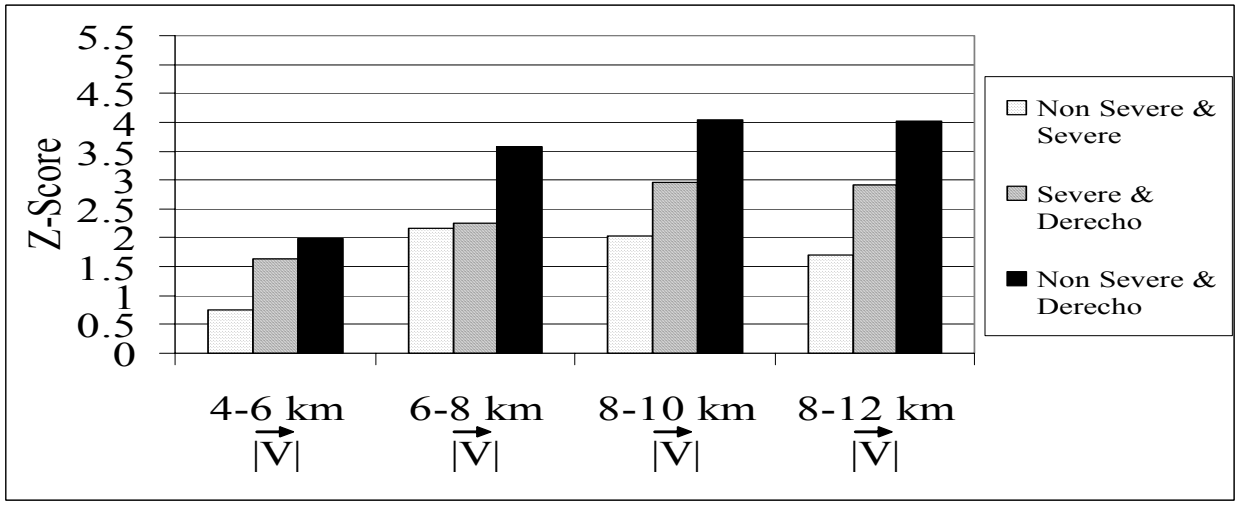

Fig. 8. Absolute values of Z-scores resulting from the Mann-Whitney test between WCSs and SCSs, SCSs and DCSs, and WCSs and DCSs for the 4-6 km, 6-8 km, 8-10 km, and 8-12 km mean wind speed .

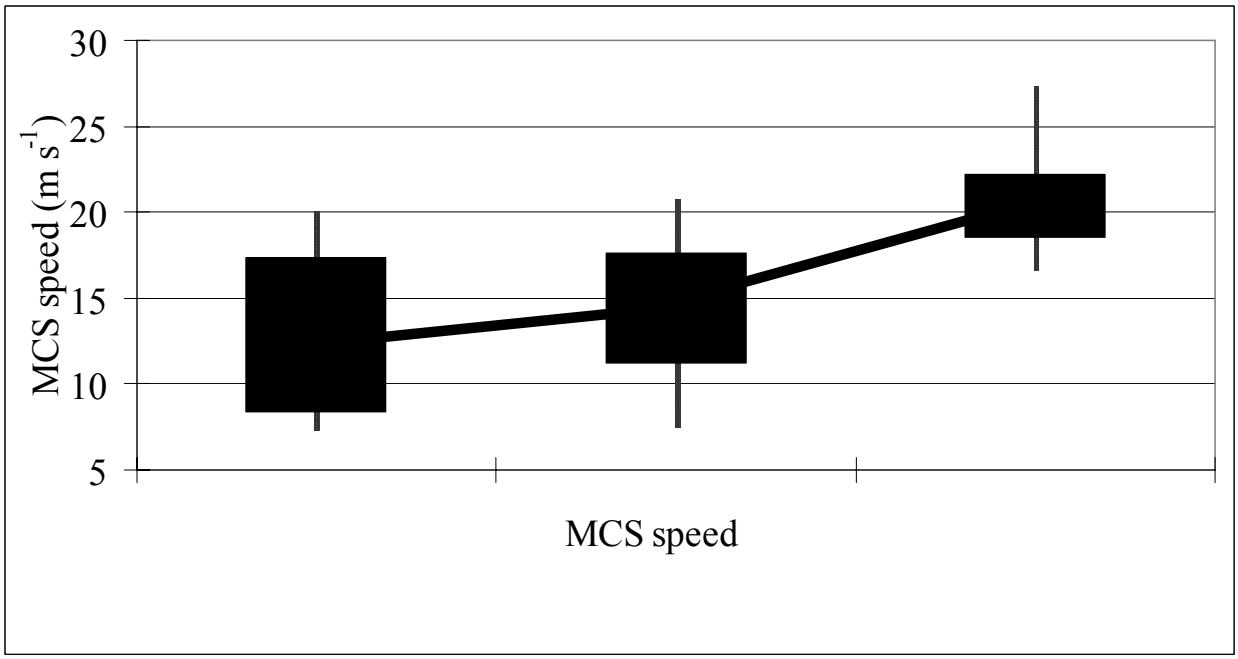

Fig. 9. Same as in Fig. 7, except for MCS speed.

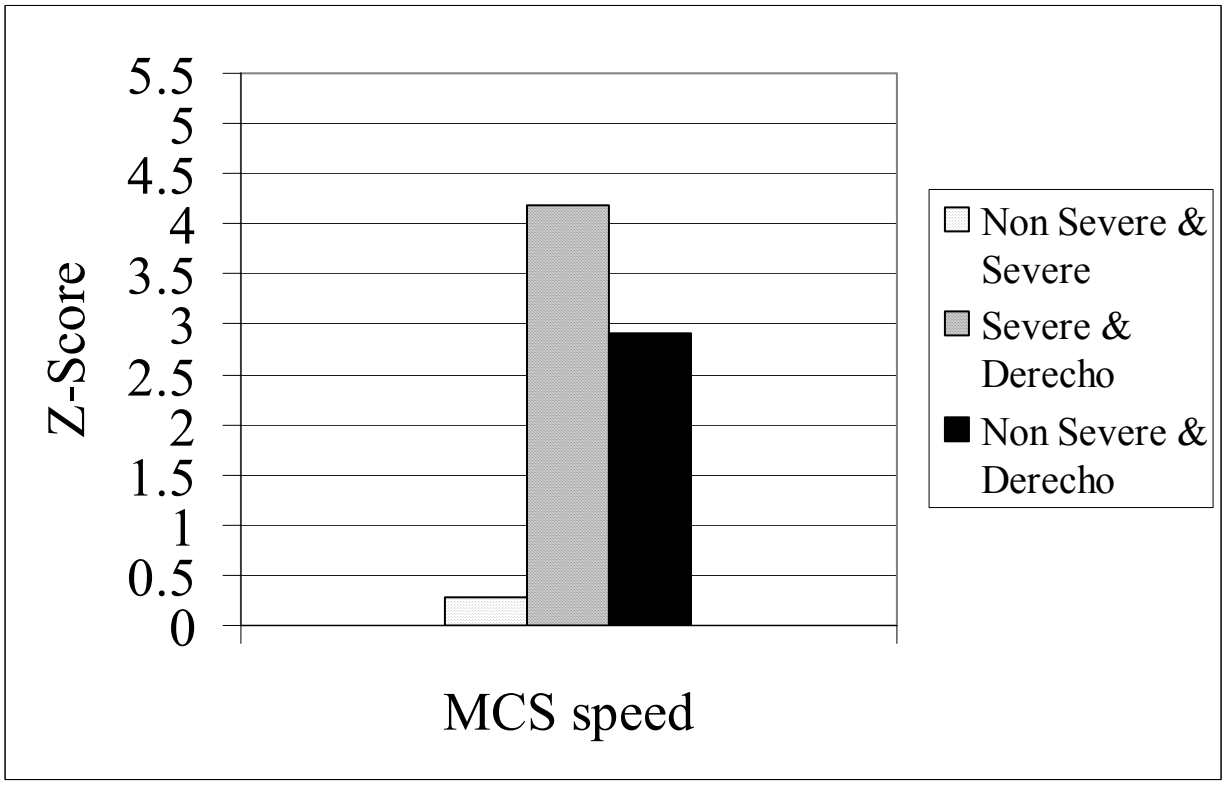

Fig. 10. Same as in Fig. 8, except for MCS speed.

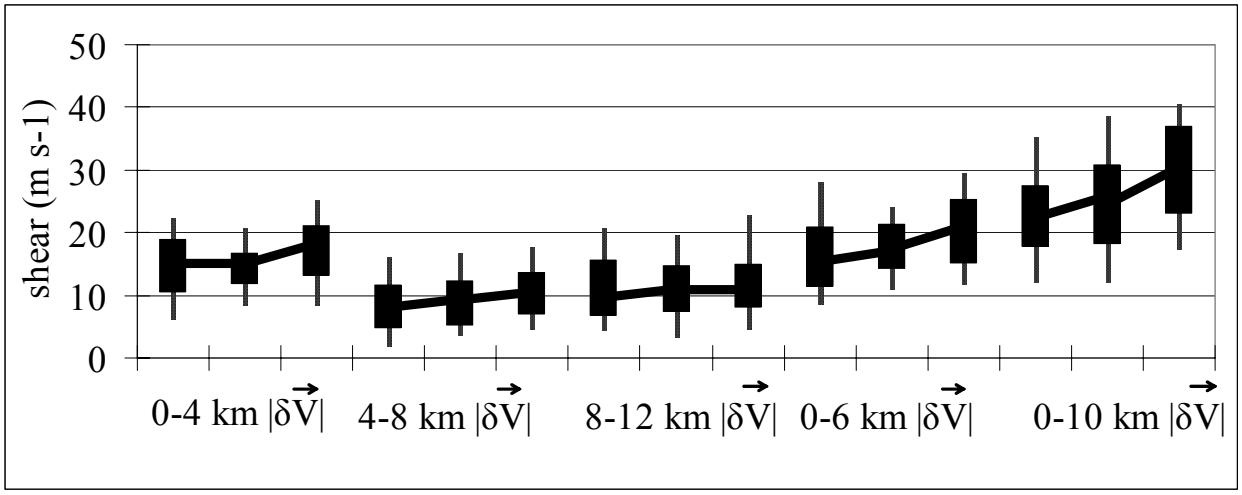

Fig. 11. Same as in Fig. 7, except for 0-4 km, 4-8 km, 8-12 km, 0-6 km, and 0-10 km bulk wind shear.

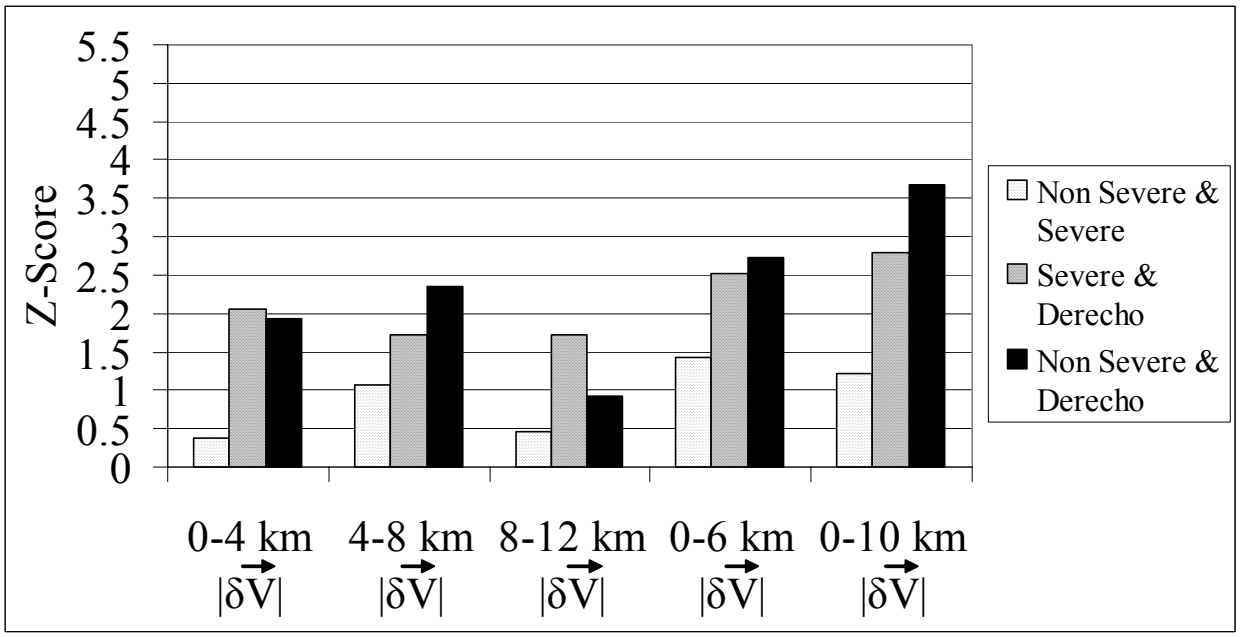

Fig. 12. Same as in Fig. 8, except for 0-4 km, 4-8 km, 8-12 km, 0-6 km, and 0-10 km bulk wind shear.

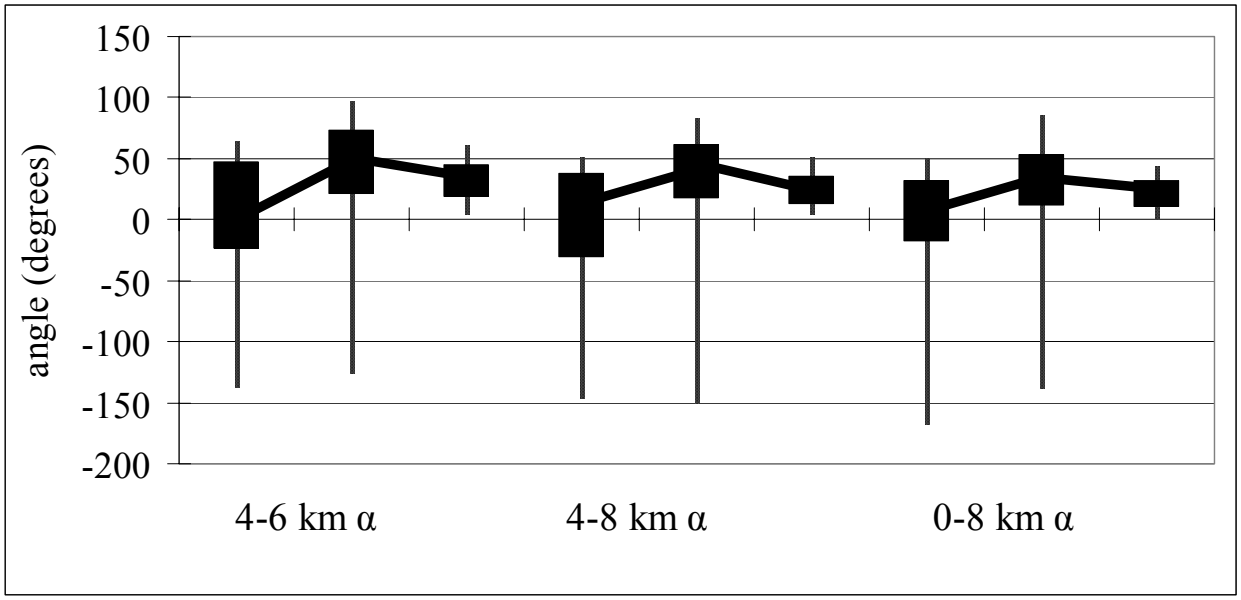

Fig. 13. Same as in Fig. 7, except for 4-6 km, 4-8 km, and 0-8 km α.

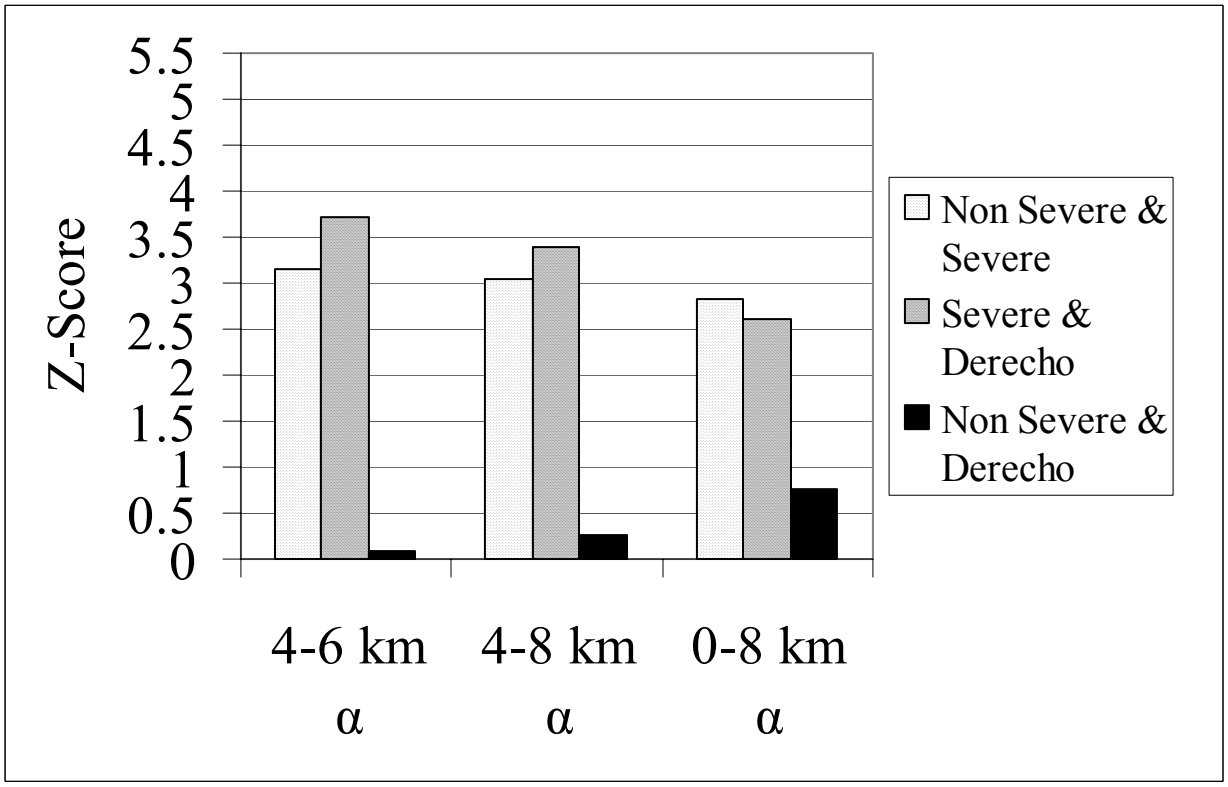

Fig. 14. Same as in Fig. 8, except for 4-6 km, 4-8 km, and 0-8 km α.

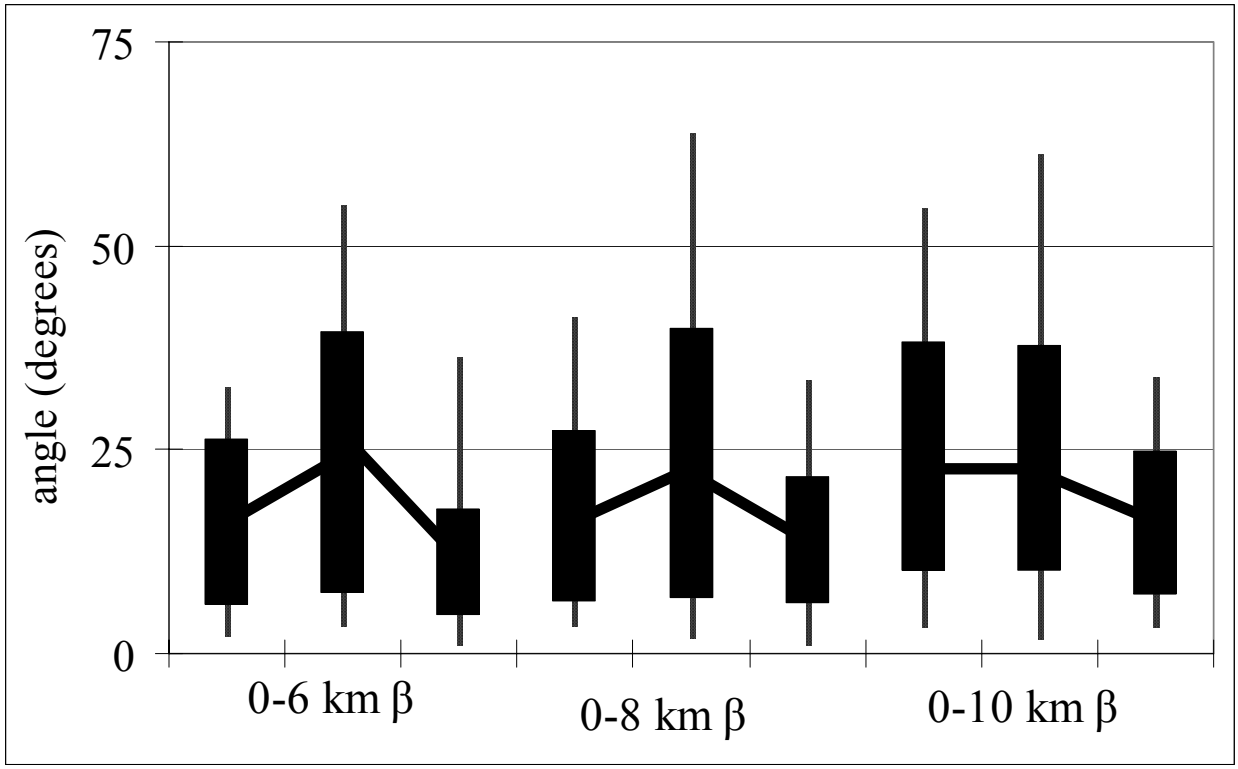

Fig. 15. Same as in Fig. 7, except for 0-6 km, 0-8 km, and 0-10 km β.

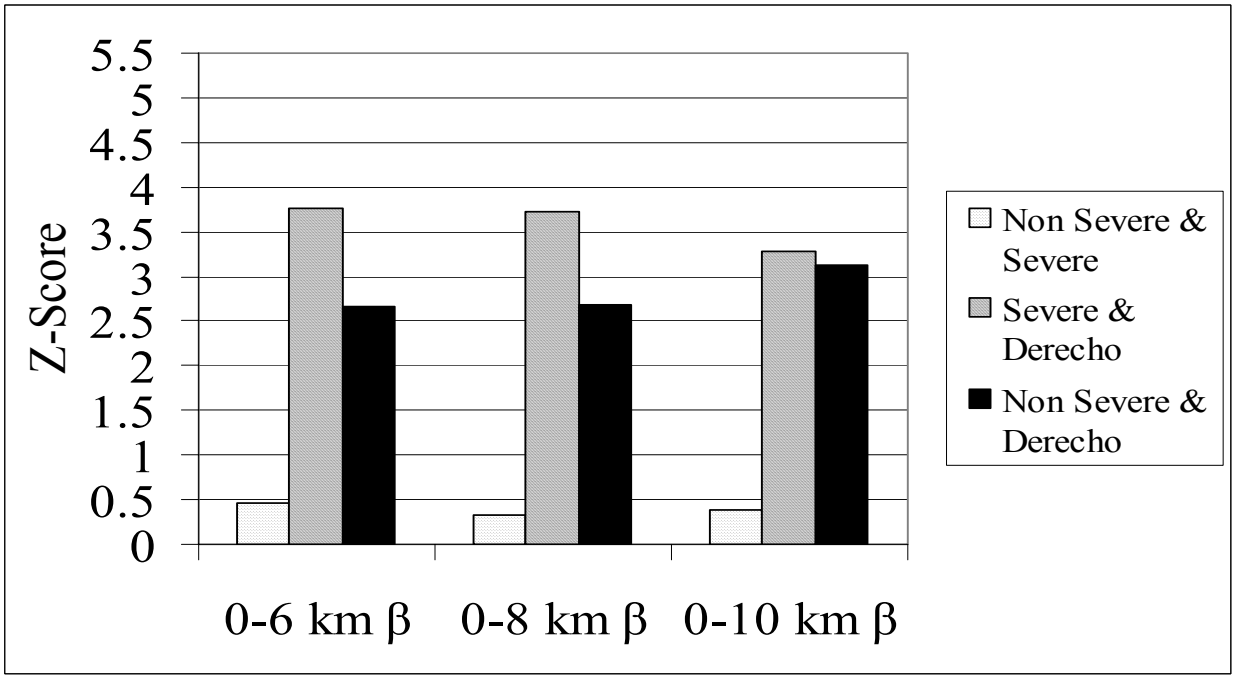

Fig. 16. Same as in Fig. 8, except for 0-6 km, 0-8 km, and 0-10 km β.

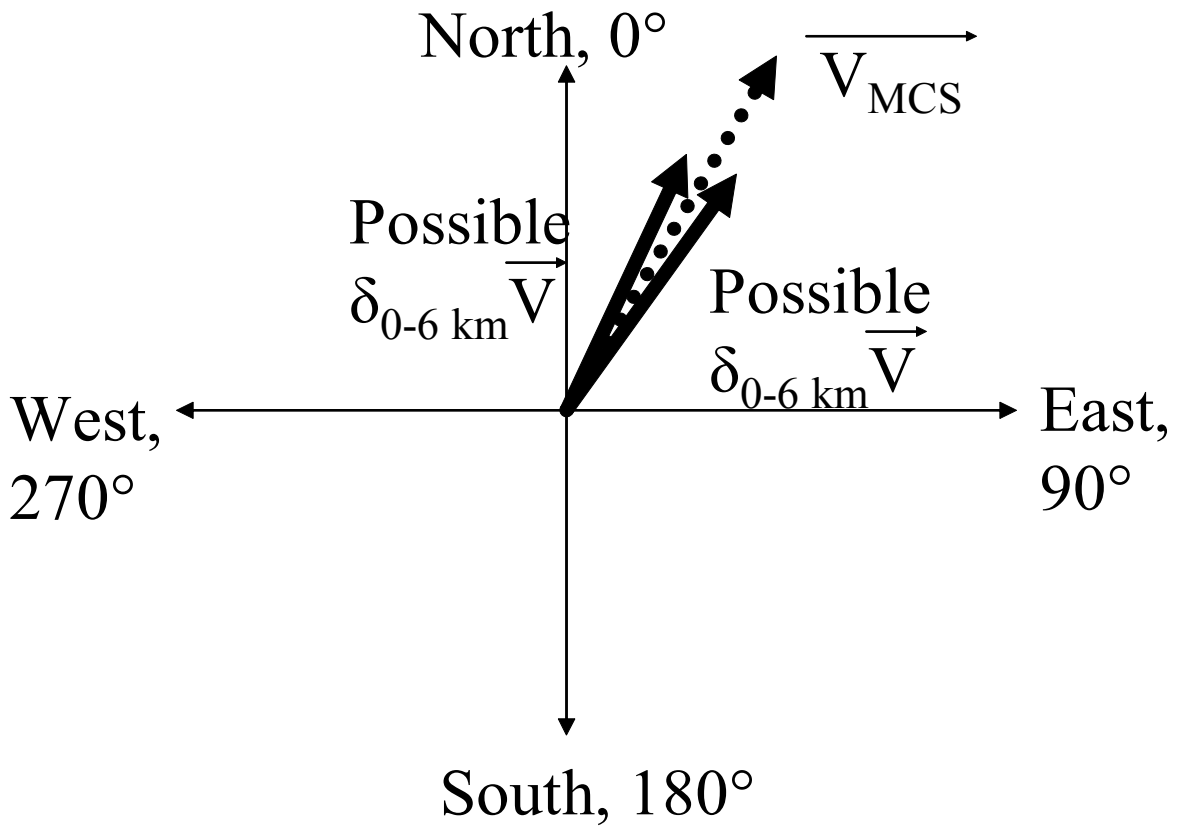

Fig. 17. The MCS motion vector, V_{MCS}, and the 0-6 km vector, $\delta_{0\text{-}6\ km}V$, on the Cartesian coordinate system, corresponding to the 12 UTC proximity sounding from Topeka, Kansas on May 5, 1998, used to describe the environment of a DCS.

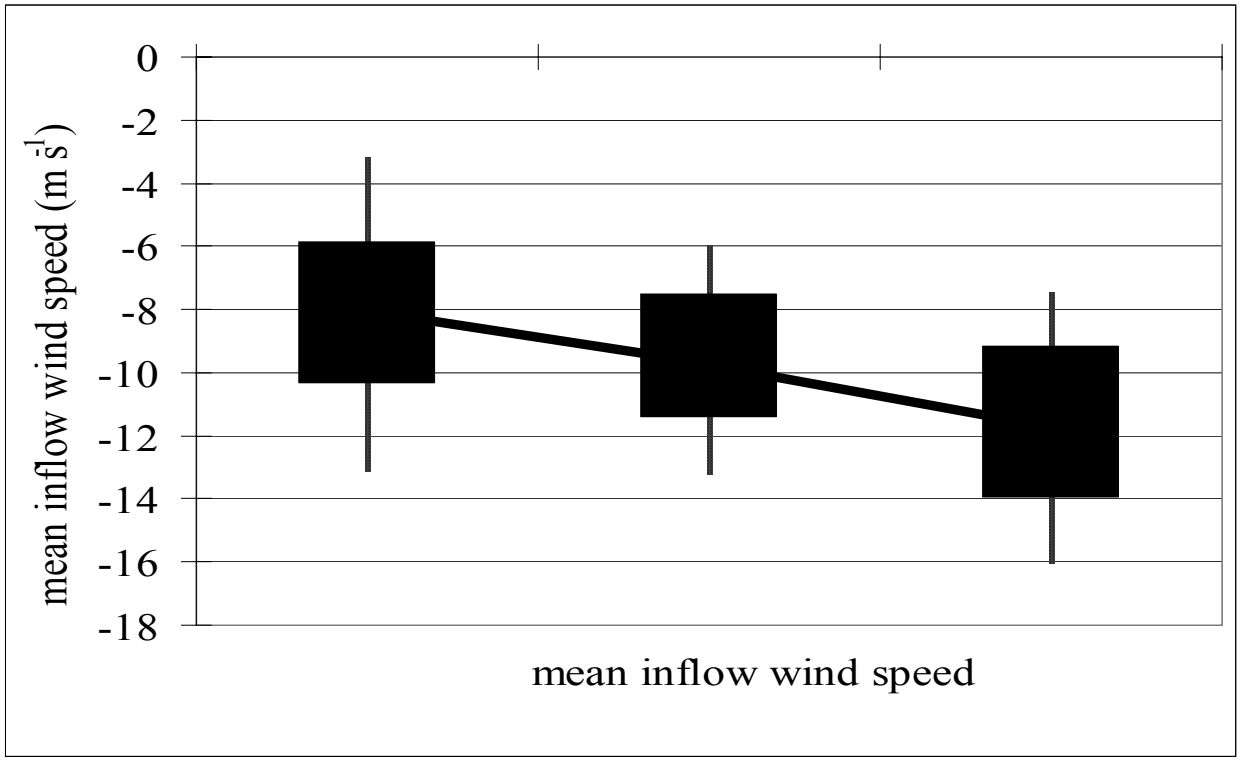

Fig. 18. Same as in Fig. 7, except for mean system-relative winds in the inflow layer.

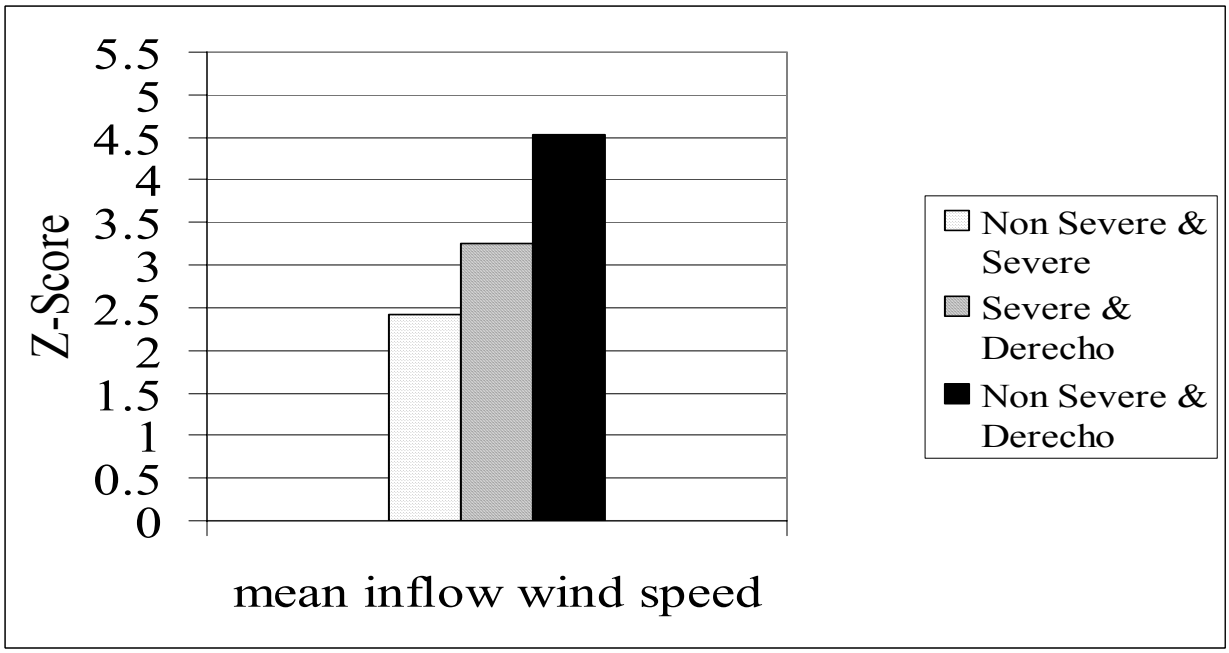

Fig. 19. Same as in Fig. 8, except for mean system-relative wind speed in the inflow layer.

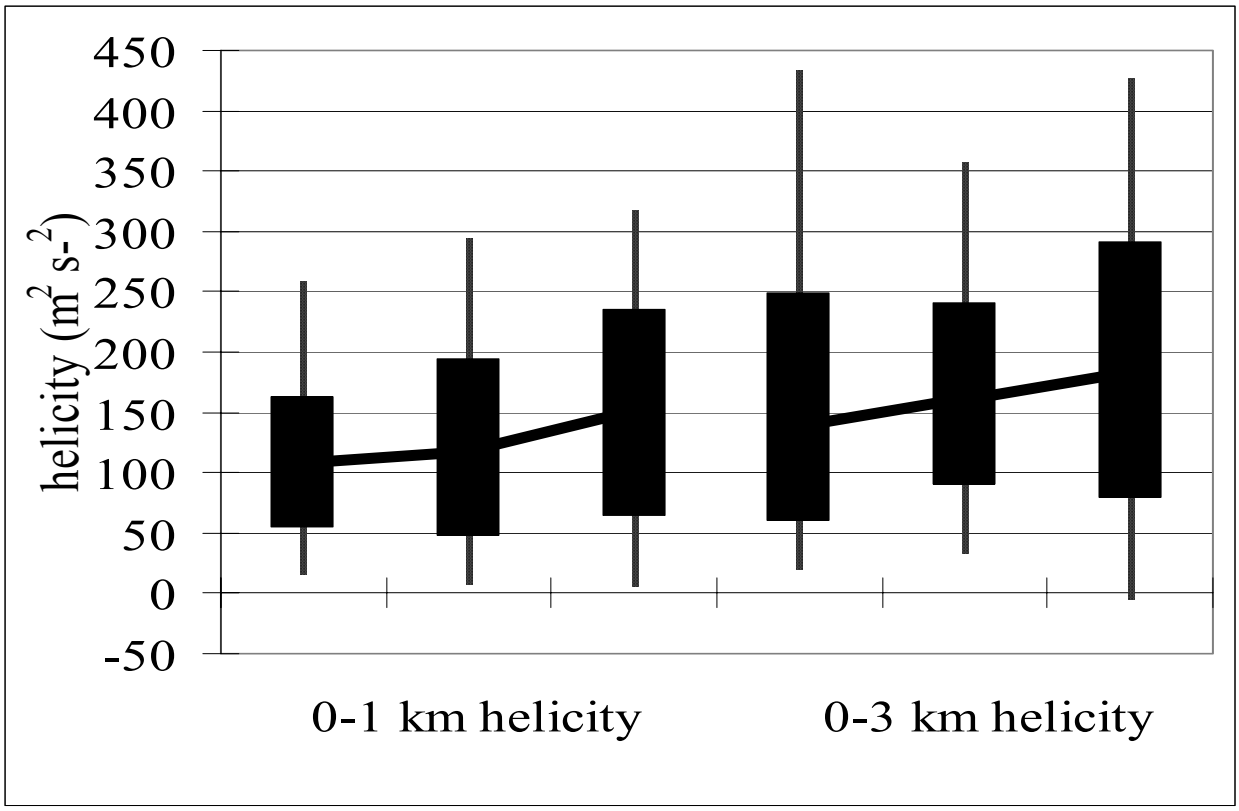

Fig. 20. Same as in Fig. 7, except for 0-1 km and 0-3 km helicity.

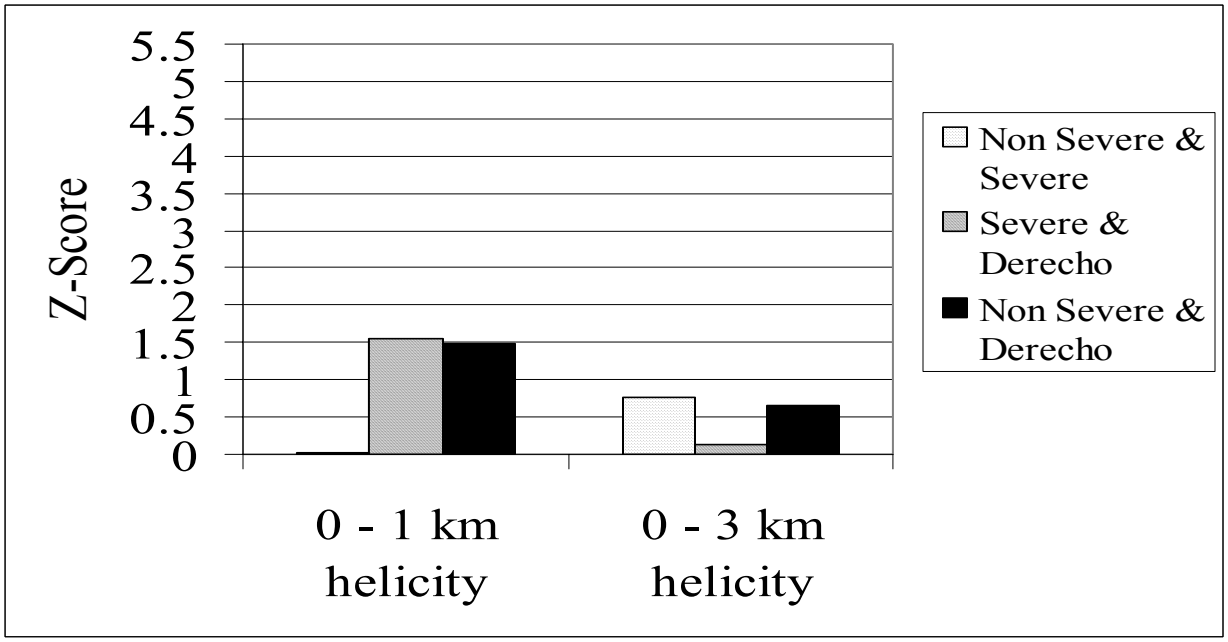

Fig. 21. Same as in Fig. 8, except for 0-1 km and 0-3 km helicity.

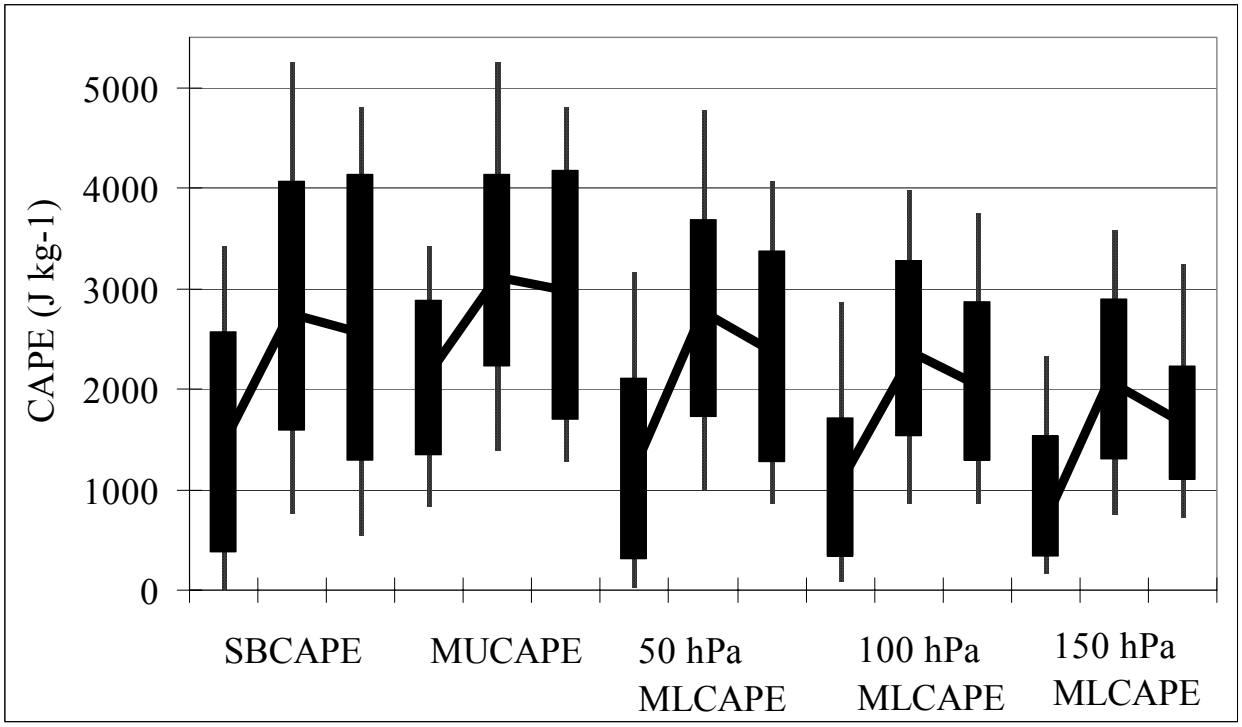

Fig. 22. Same as in Fig. 7, except for SBCAPE, MUCAPE, and 50 hPa, 100 hPa, and 150 hPa MLCAPE.

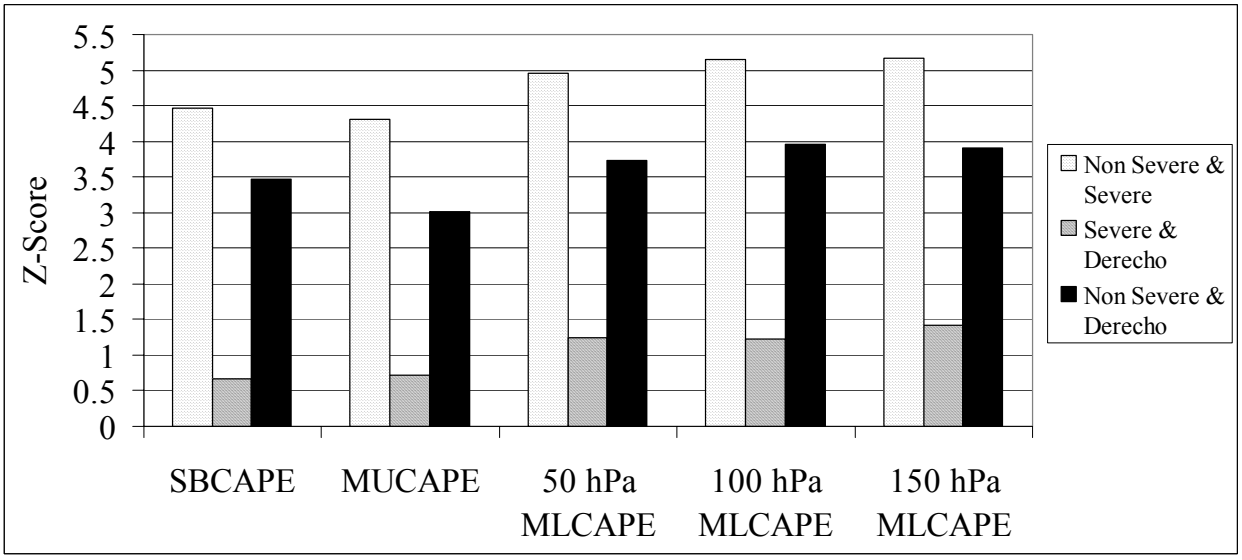

Fig. 23. Same as in Fig. 8, except for SBCAPE, MUCAPE, and 50 hPa, 100 hPa, and 150 hPa MLCAPE.

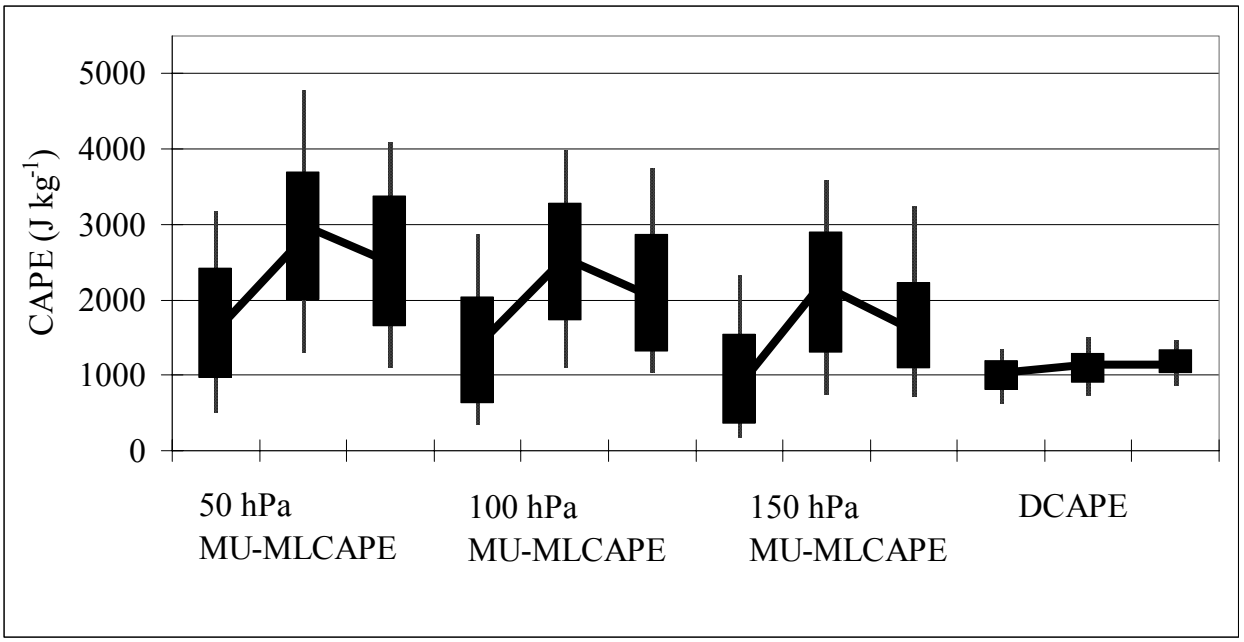

Fig. 24. Same as in Fig. 7, except for 50 hPa, 100 hPa, and 150 hPa MU-MLCAPE and DCAPE.

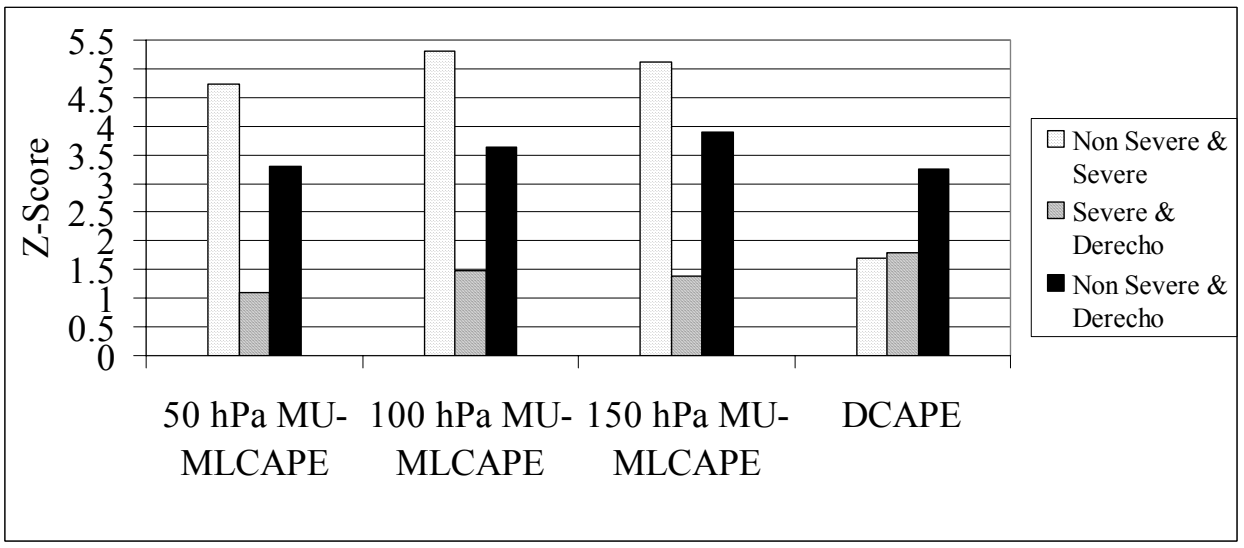

Fig. 25. Same as in Fig. 8, except for 50 hPa, 100 hPa, and 150 hPa MU-MLCAPE and DCAPE.

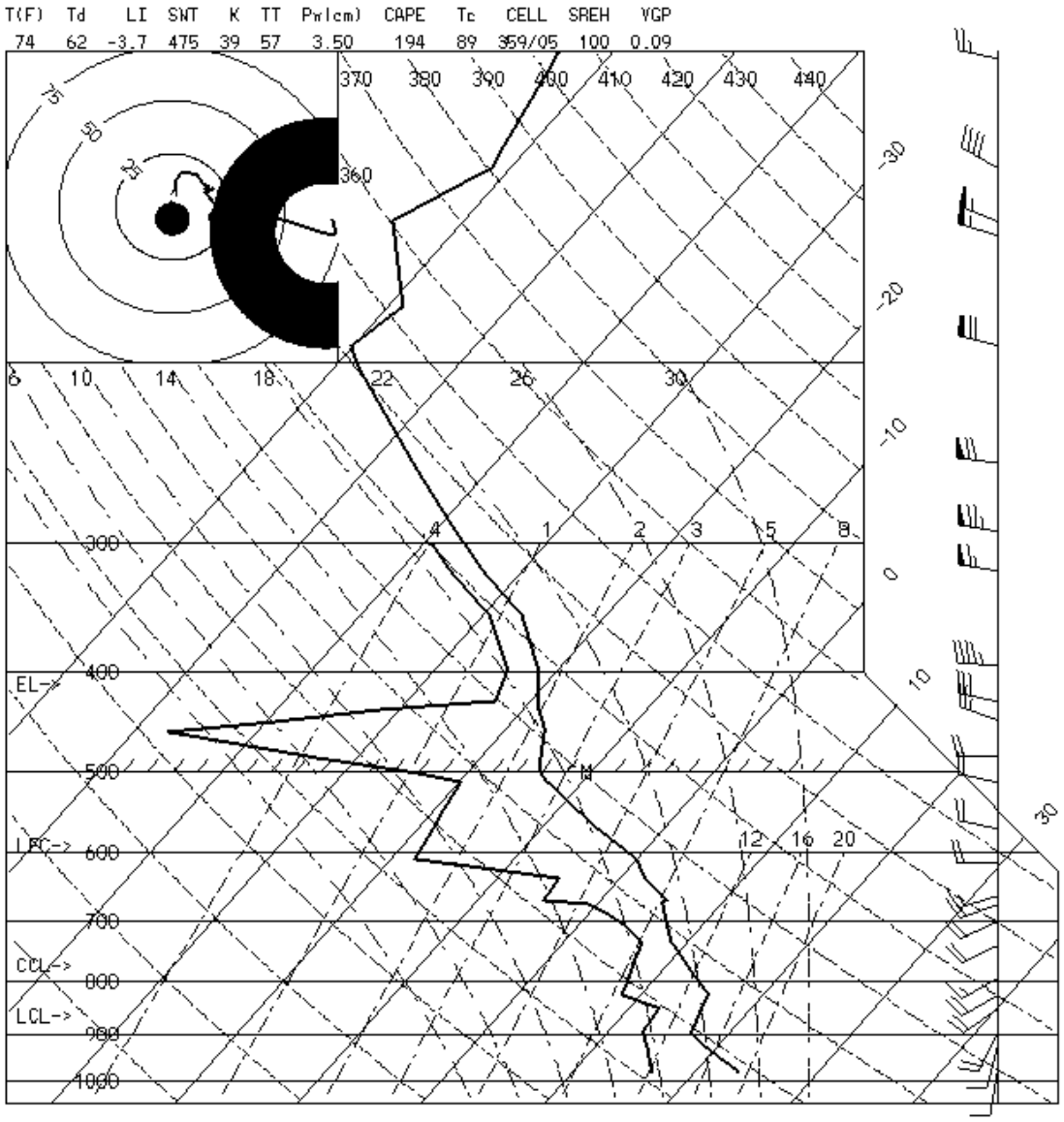

Fig. 26. 00 UTC radiosonde data from August 23, 2000 at Detroit.

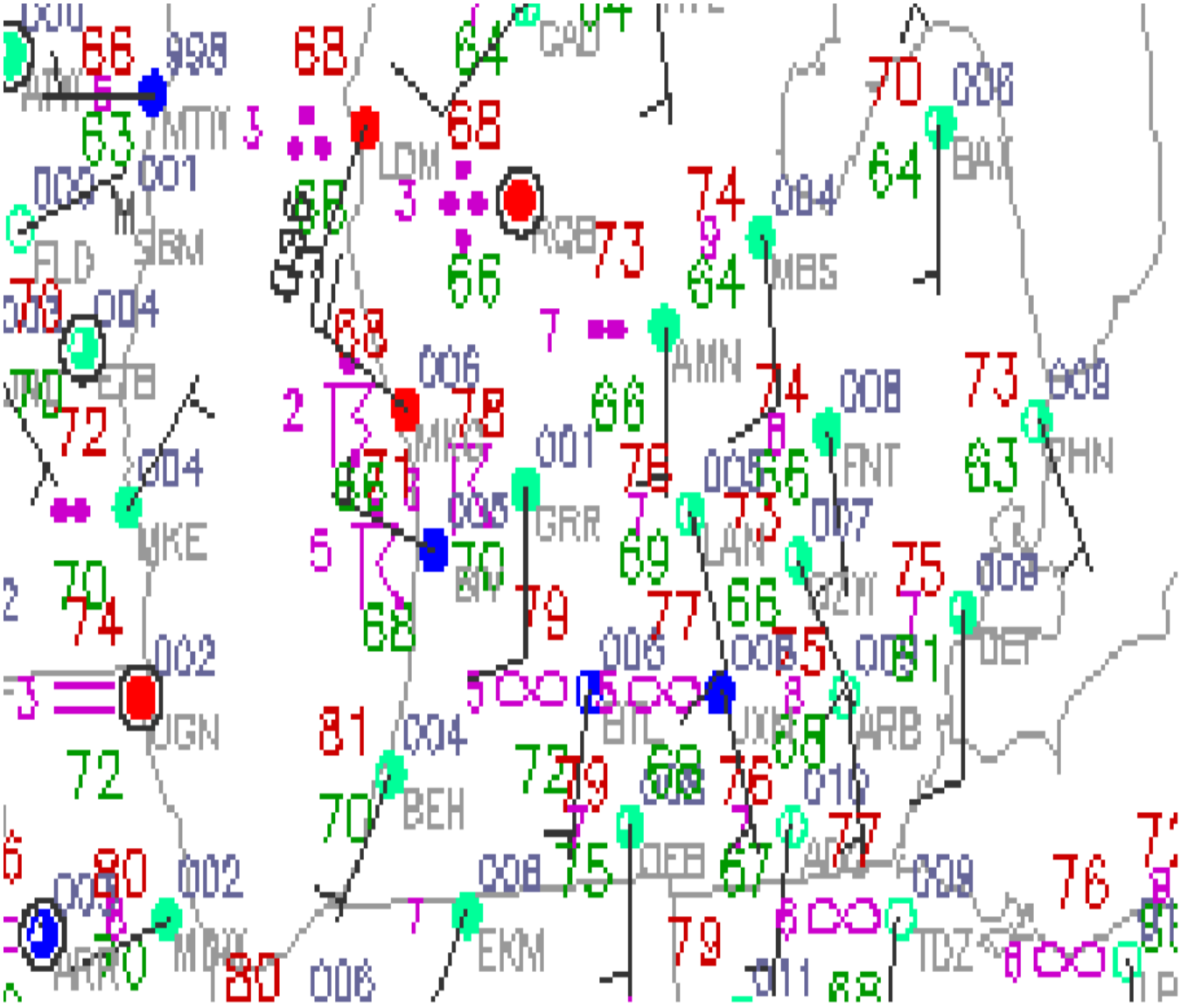

Fig. 27. 00 UTC surface observations across Lower Michigan on August 23, 2000.

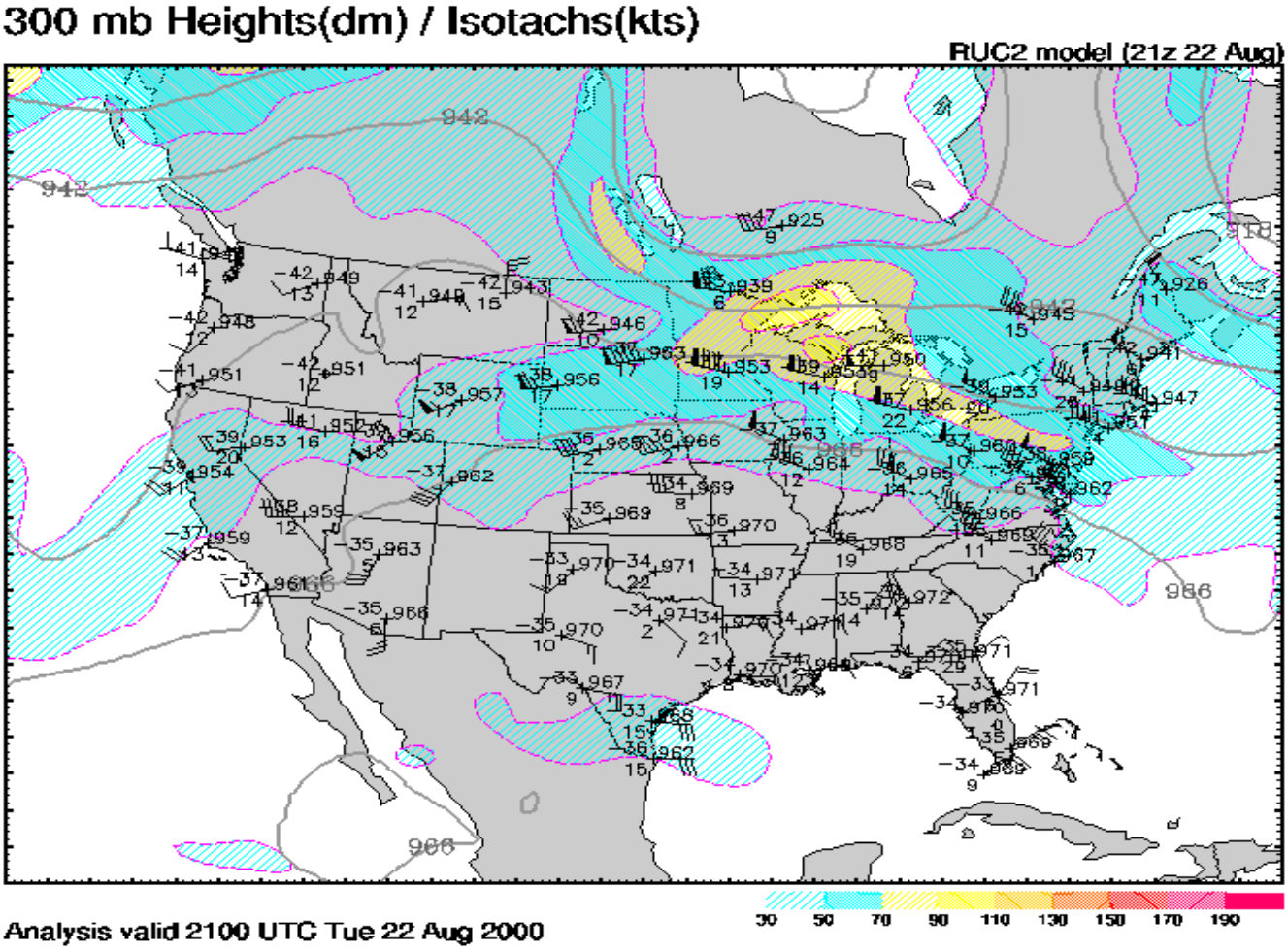

Fig. 28. 21 UTC 300 mb chart on August 22, 2000.

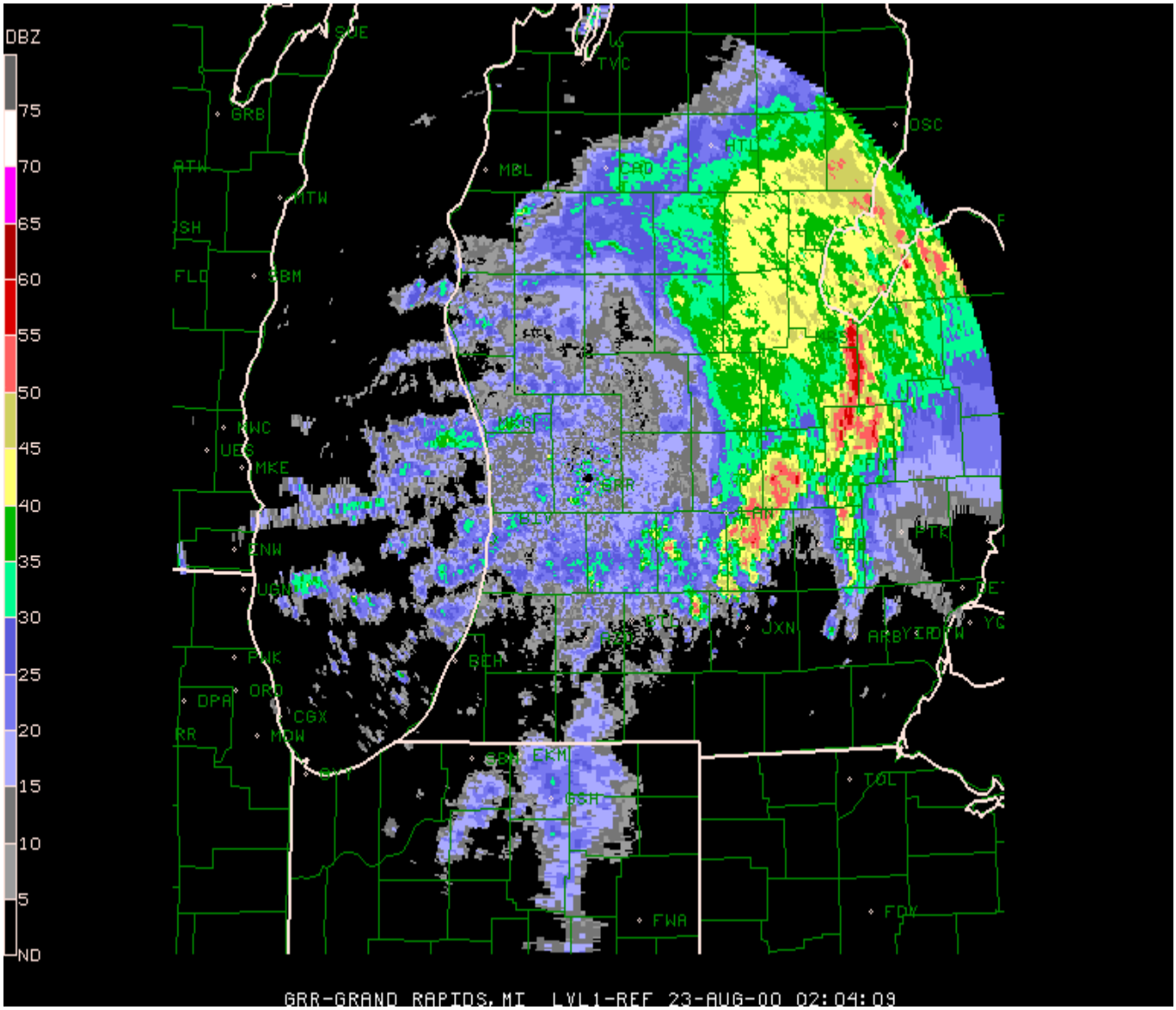

Fig. 29. 0204 UTC base-reflectivity data from Grand Rapids, Michigan on August 23, 2000.

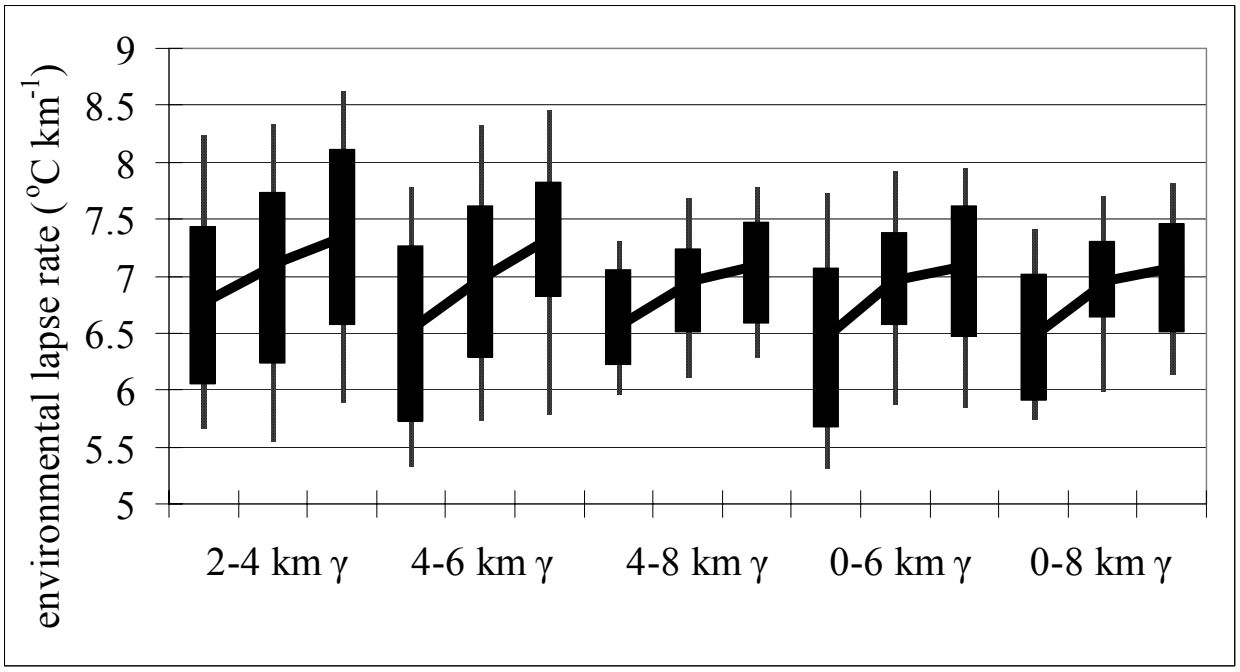

Fig. 30. Same as in Fig. 7, except for 2-4 km, 4-6 km, 4-8 km, 0-6 km, and 0-8 km γ.

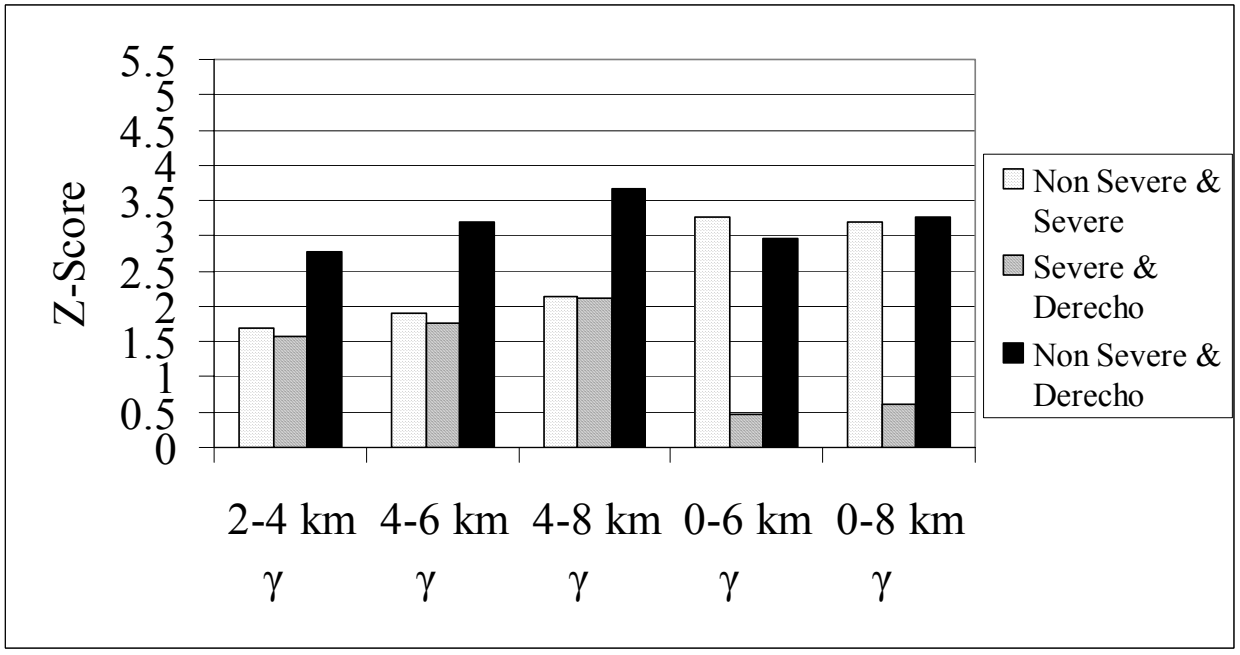

Fig. 31. Same as in Fig. 8, except for 2-4 km, 4-6 km, 4-8 km, 0-6 km, and 0-8 km γ.

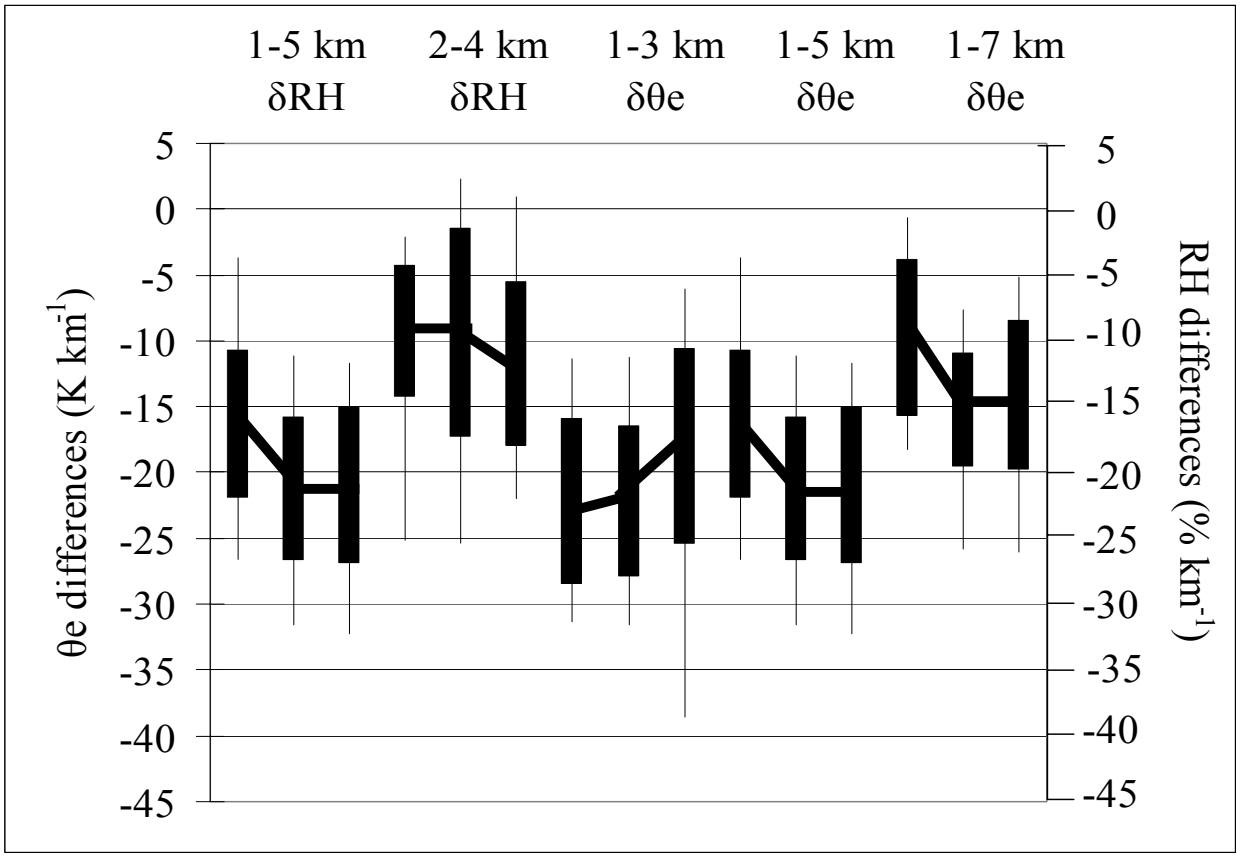

Fig. 32. Same as in Fig. 7, except for 1-3 km, 1-5 km, and 1-7 km vertical moisture differences.

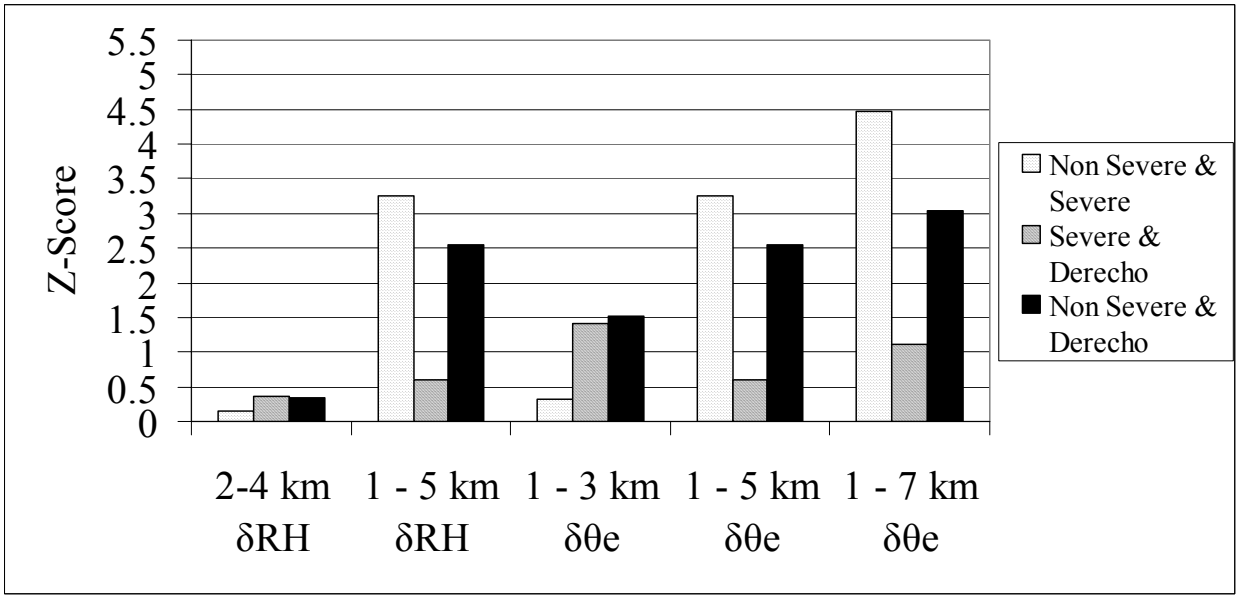

Fig. 33. Same as in Fig. 8, except for 1-3 km, 1-5 km, and 1-7 km vertical moisture differences.

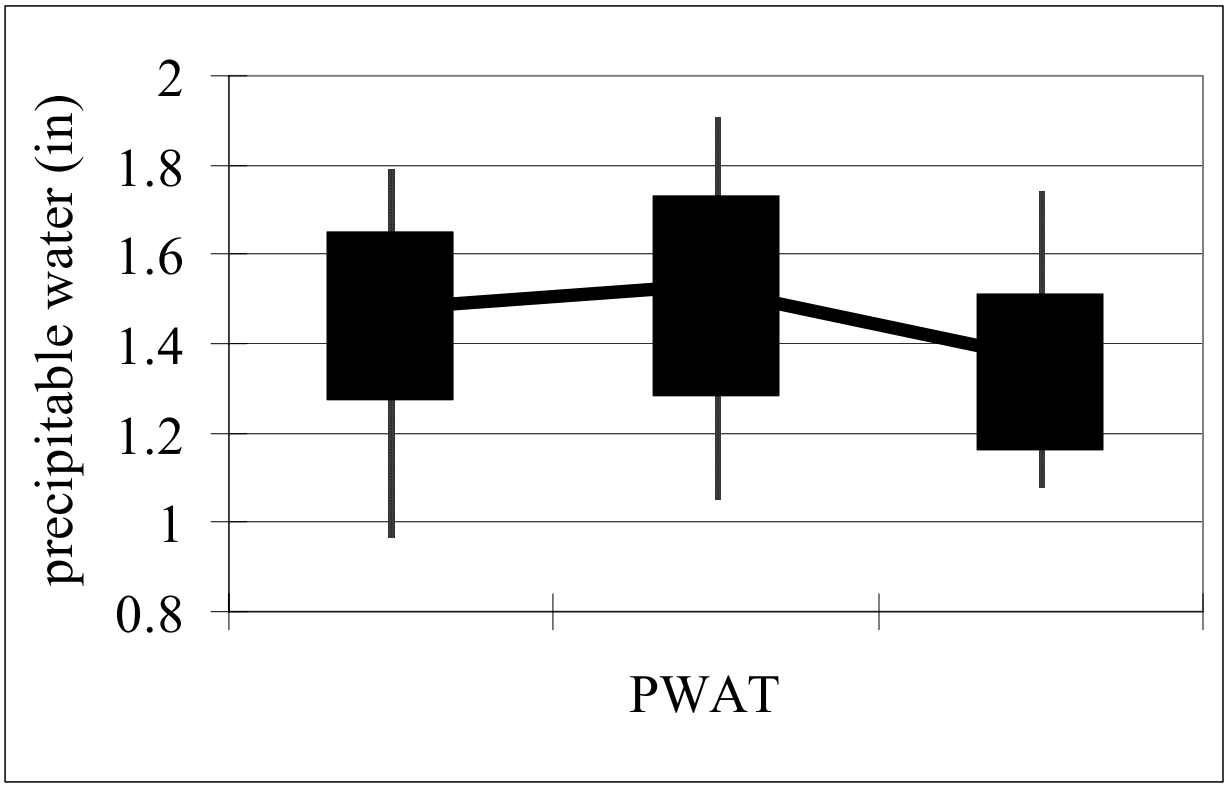

Fig. 34. Same as in Fig.2, except for PWAT.

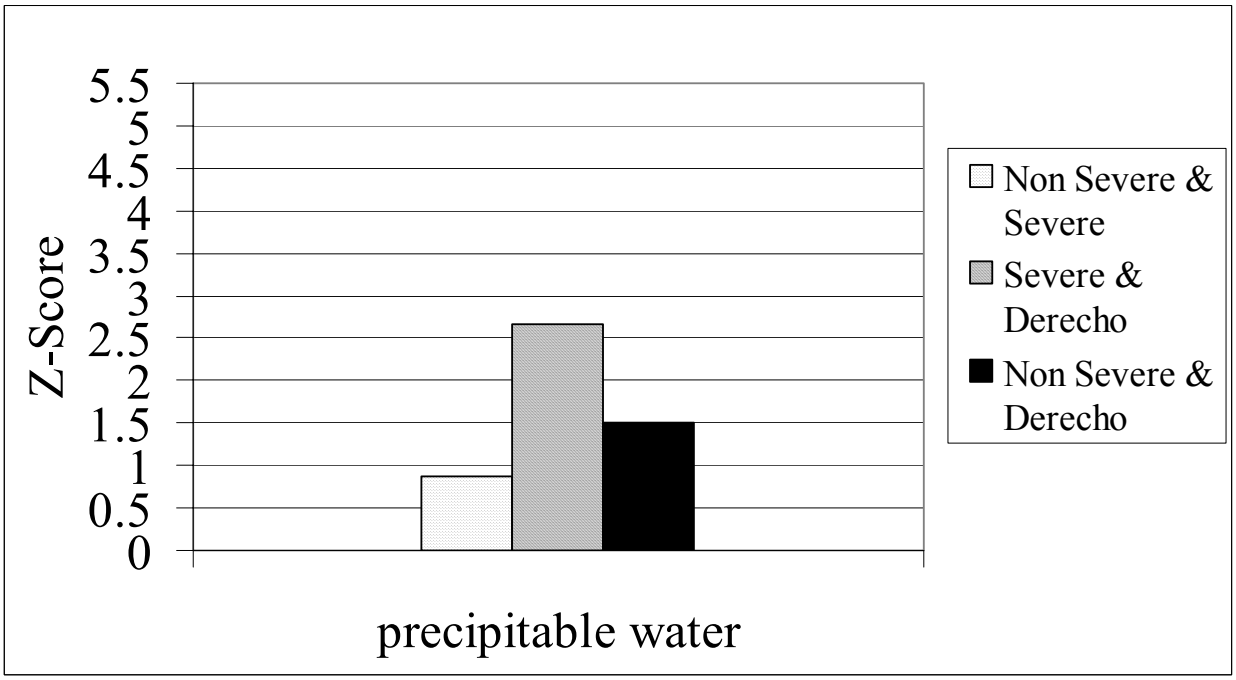

Fig. 35. Same as in Fig. 8, except for PWAT.